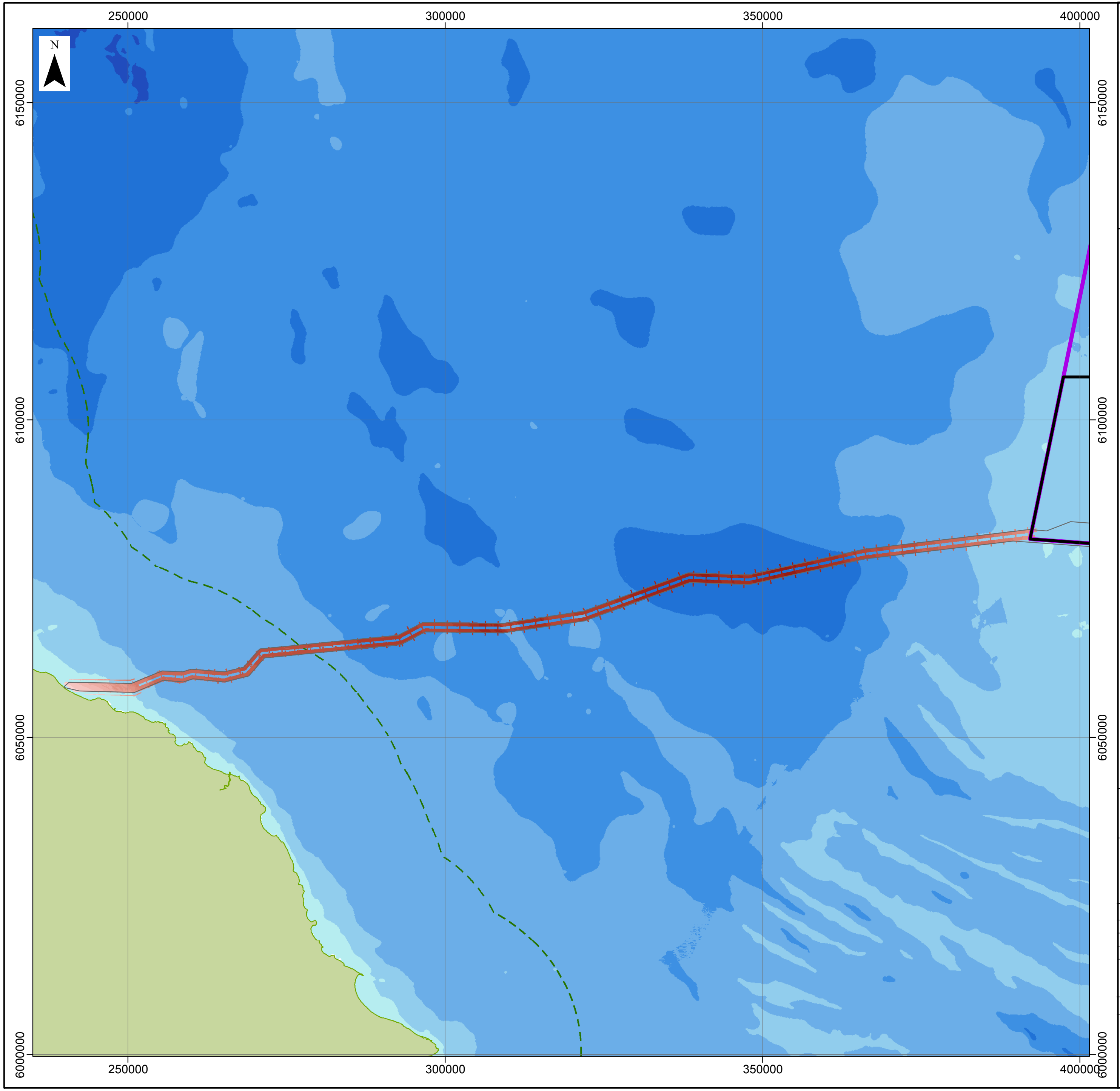

LEGEND

- ▭ Dogger Bank Zone
- ▭ Tranche A Boundary
- ▭ Teesside_CableCorrid...
- - - - 12nm Territorial Boundary

Bathymetry (m below LAT)

▨ Above 0	▨ 30 - 35
▨ 0 - 5	▨ 35 - 40
▨ 5 - 10	▨ 40 - 45
▨ 10 - 15	▨ 45 - 50
▨ 15 - 20	▨ 50 - 55
▨ 20 - 25	▨ 55 - 60
▨ 25 - 30	▨ 60 - 65
	▨ 65 - 70
	▨ 70 - 75
	▨ 75 - 80
	▨ 80 - 85
	▨ 85 - 90

0 40
Kilometres

Data Source:
Survey Bathymetry © Gardline, 2013,
Background bathymetry image derived in part from TCarta data © 2009

PROJECT TITLE

DOGGER BANK TEESSIDE

DRAWING TITLE

Figure 3.1 Export Cable Corridor Bathymetry

VER	DATE	REMARKS	Drawn	Checked
1	25/04/2013	Draft	FK	DB
2	20/03/2014	Final	GC	DB

DRAWING NUMBER: **9X5889/04/050**

SCALE	1:900,000	PLOT SIZE	A4	DATUM	WGS84	PROJECTION	UTM 31N

FOREWIND

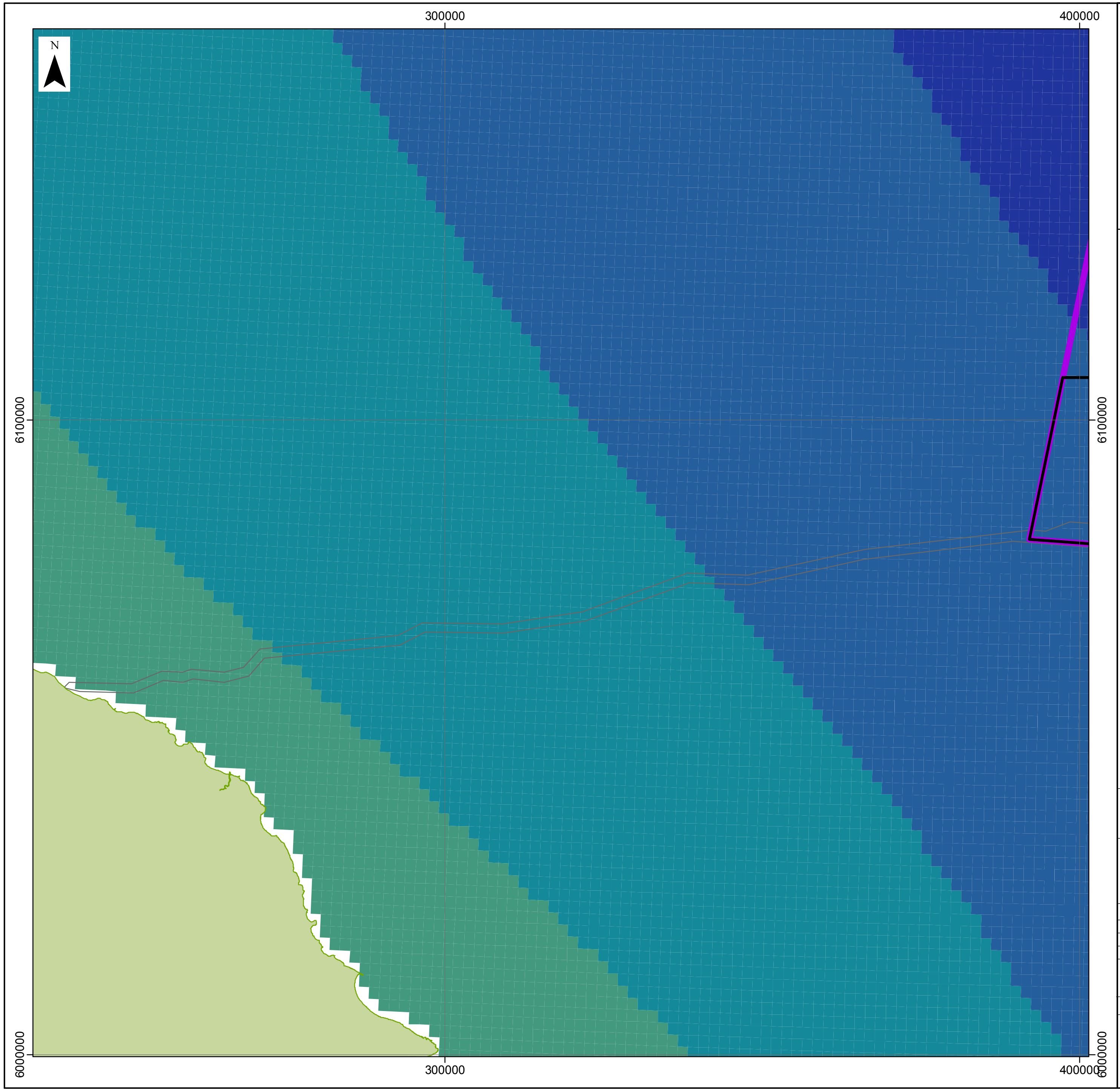

LEGEND

- ▭ Dogger Bank Zone
- ▭ Tranche A Boundary
- ☐ Dogger Bank Teesside A & B Export Cable Corridor

Mean Spring Tide Range (m)

- 🟦 1.01 - 2.00
- 🟦 2.01 - 3.00
- 🟦 3.01 - 4.00
- 🟩 4.01 - 5.00

0 20
Kilometres

Data Source:
BERR (http://www.renewables-atlas.info/)

PROJECT TITLE

DOGGER BANK TEESSIDE A & B

DRAWING TITLE

Figure 3.2 Spring Tidal Range across the Dogger Bank Teesside A and B Export Cable Corridor

VER	DATE	REMARKS	Drawn	Checked
1	10/12/2012	Draft	FK	DB
2	15/10/2013	Final	LW	DB

DRAWING NUMBER: **9X5889/04/042**

SCALE	1:900,000	PLOT SIZE	A4	DATUM	WGS84	PROJECTION	UTM31N

FOREWIND

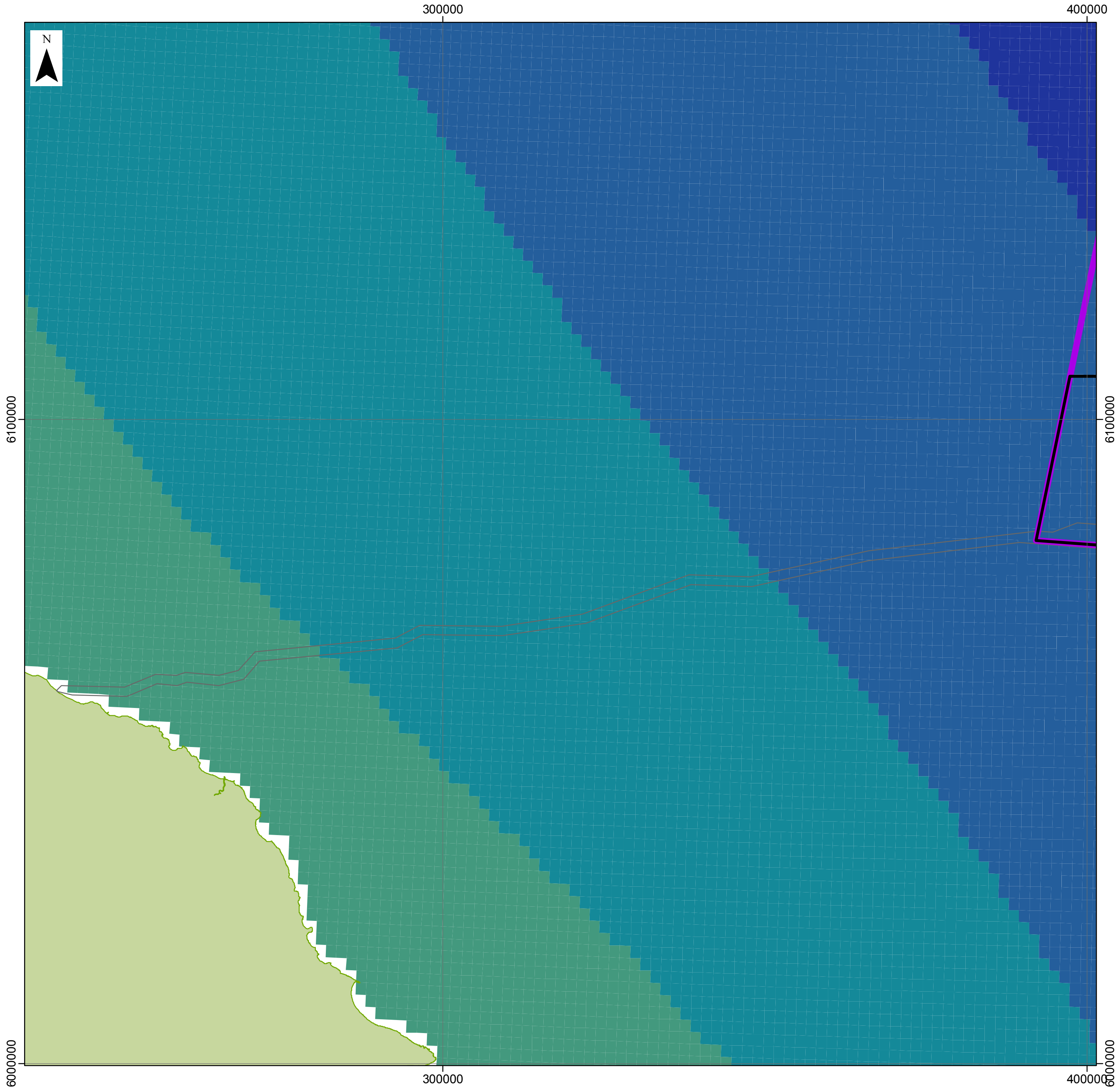

LEGEND

▭ Dogger Bank Zone

▭ Tranche A Boundary

▭ Dogger Bank Teesside A & B Export Cable Corridor

Mean Neap Tide Range (m)

🟦	0.51 - 1.00
🟦	1.01 - 1.50
🟦	1.51 - 2.00
🟩	2.01 - 2.50

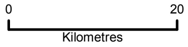

Data Source:
BERR (http://www.renewables-atlas.info/)

PROJECT TITLE

DOGGER BANK TEESSIDE A & B

DRAWING TITLE

Figure 3.3 Neap Tidal Range across the Dogger Bank Teesside A and B Export Cable Corridor

VER	DATE	REMARKS	Drawn	Checked
1	10/12/2012	Draft	FK	DB
2	15/10/2013	Final	LW	DB

DRAWING NUMBER: **9X5889/04/043**

SCALE	1:900,000	PLOT SIZE	A4	DATUM	WGS84	PROJECTION	UTM31N

FOREWIND

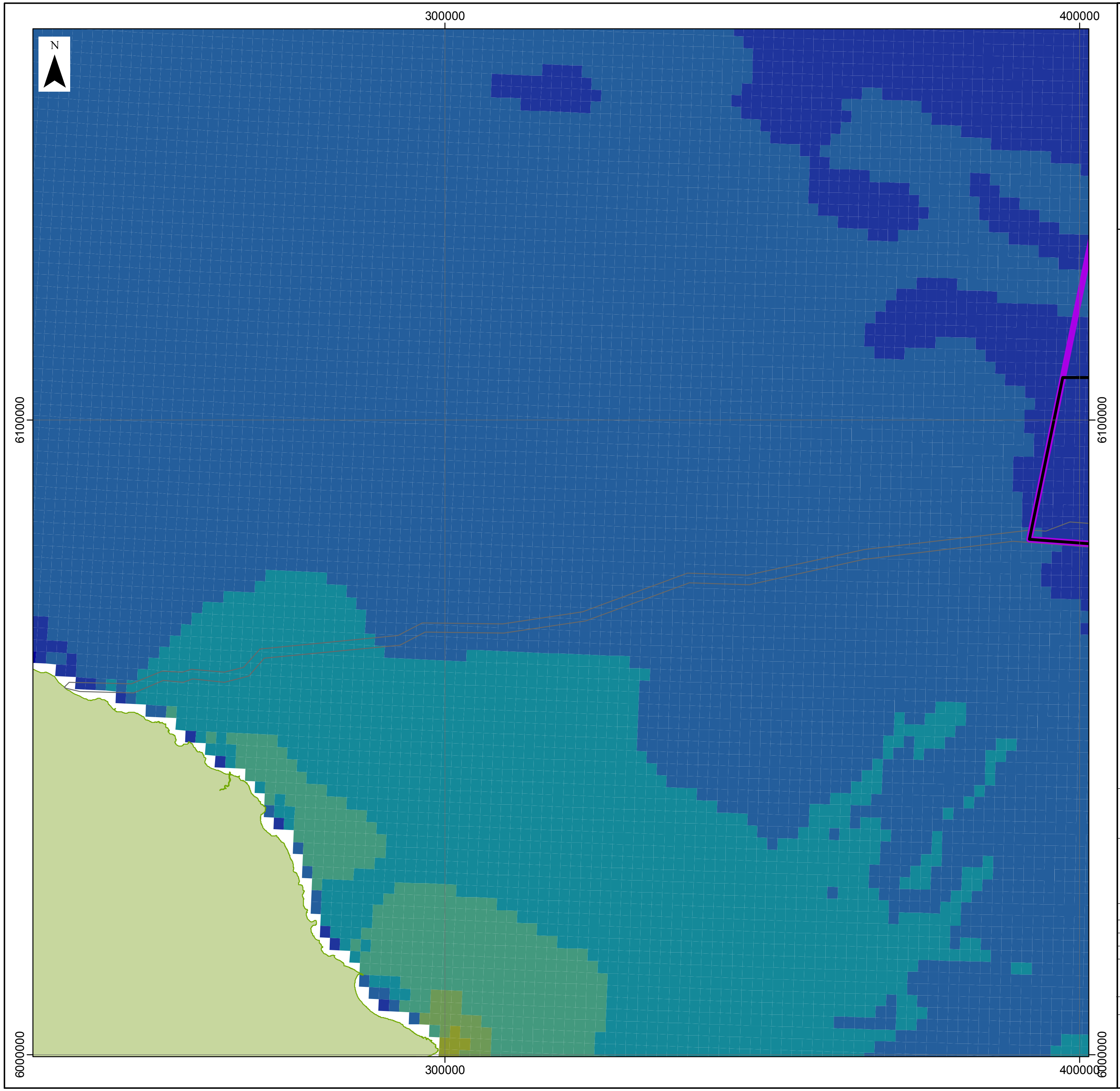

LEGEND

▭ Dogger Bank Zone
▭ Tranche A Boundary
☐ Dogger Bank Teesside A & B Export Cable Corridor

Peak Flow of Mean Spring Tide (m/s)

■ < 0.20
■ 0.21 - 0.40
■ 0.41 - 0.60
■ 0.61 - 0.80
■ 0.81 - 1.00
■ 1.01 - 1.20
■ 1.21 - 1.40

0 20
Kilometres

Data Source:
BERR (http://www.renewables-atlas.info/)

PROJECT TITLE

DOGGER BANK TEESSIDE A & B

DRAWING TITLE

Figure 3.4 Peak Flow for a Mean Spring Tide across the Dogger Bank Teesside A and B Export Cable Corridor

VER	DATE	REMARKS	Drawn	Checked
1	10/12/2012	Draft	FK	DB
2	15/10/2013	Final	LW	DB

DRAWING NUMBER: **9X5889/04/044**

SCALE	1:900,000	PLOT SIZE	A4	DATUM	WGS84	PROJECTION	UTM31N

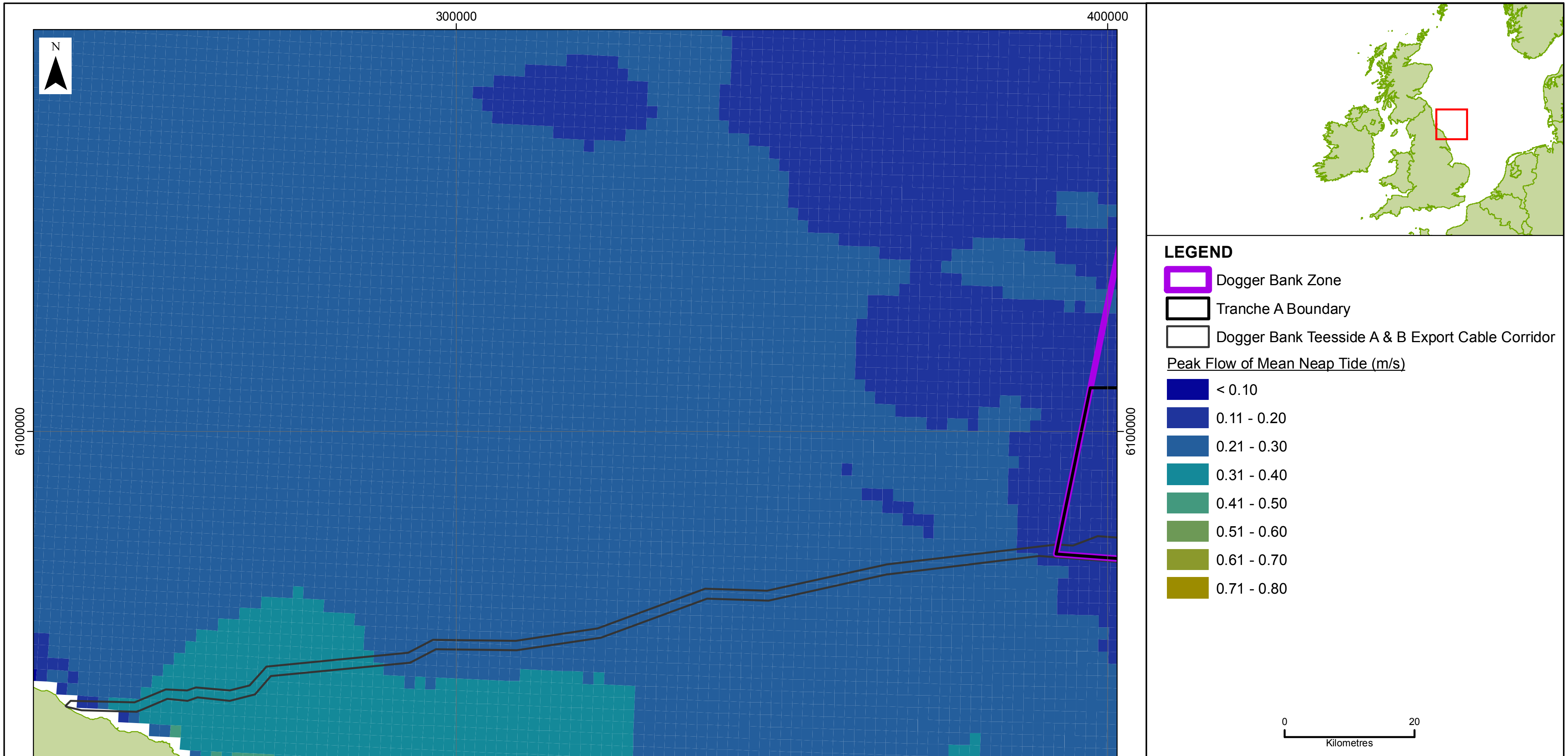

Data Source:
BERR (http://www.renewables-atlas.info/)

PROJECT TITLE

DOGGER BANK TEESSIDE A & B

DRAWING TITLE

Figure 3.5 Peak Flow for a Mean Neap Tide across the Dogger Bank Teesside A and B Export Cable Corridor

VER	DATE	REMARKS	Drawn	Checked
1	10/12/2012	Draft	FK	DB
2	15/10/2013	Final	LW	DB

DRAWING NUMBER: **9X5889/04/45**

SCALE	1:900,000	PLOT SIZE	A4	DATUM	WGS84	PROJECTION	UTM31N

FOREWIND

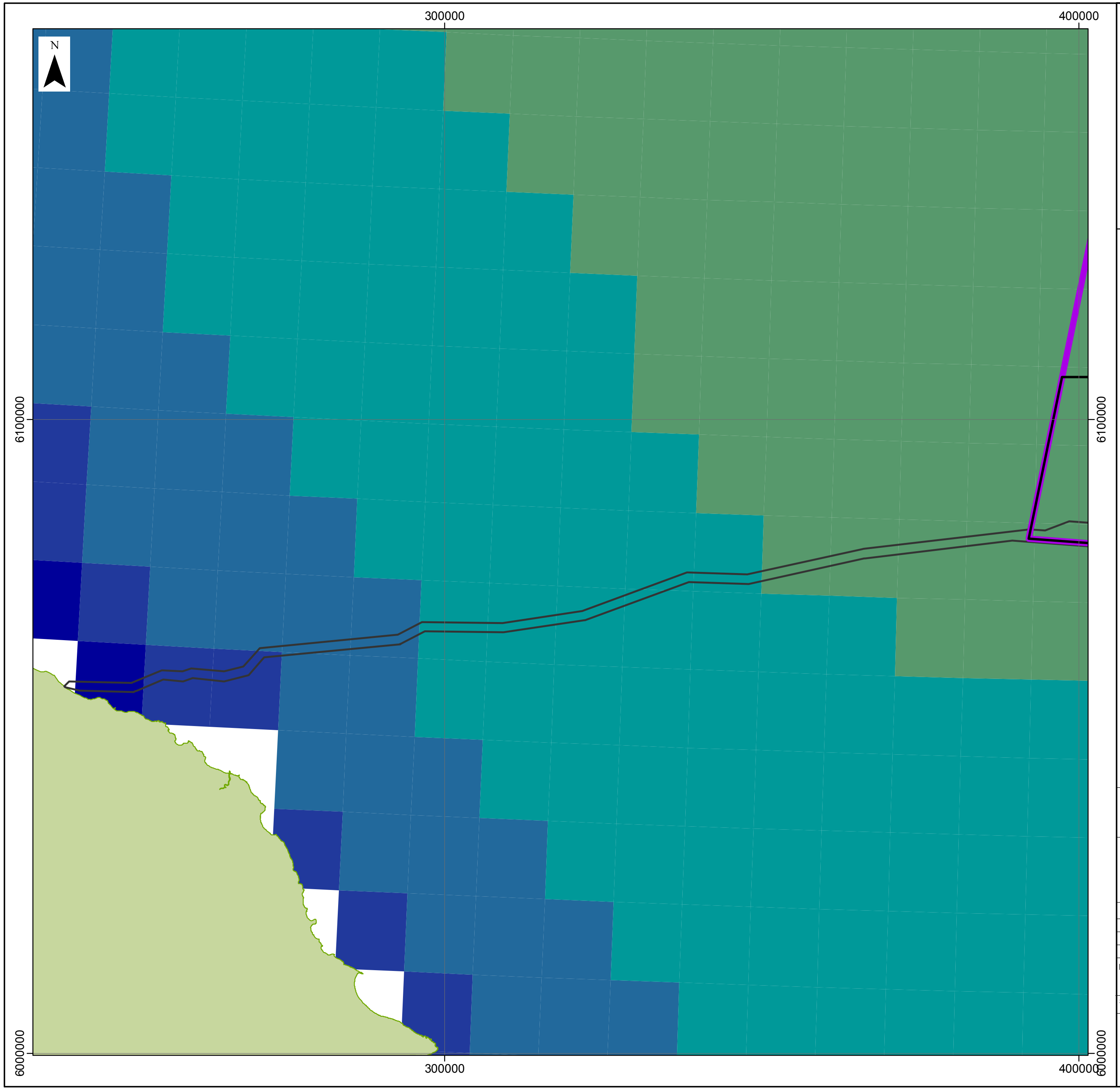

LEGEND

▭ Dogger Bank Zone
▭ Tranche A Boundary
▭ Dogger Bank Teesside A & B Export Cable Corridor

Annual Mean Significant Wave Height (m)

■ < 1.00
■ 1.01 - 1.25
■ 1.26 - 1.50
■ 1.51 - 1.75
■ 1.76 - 2.00

0 20
Kilometres

Data Source:
BERR (http://www.renewables-atlas.info/)

PROJECT TITLE

DOGGER BANK TEESSIDE A & B

DRAWING TITLE

Figure 3.6 Annual Mean Significant Wave Height Across the Dogger Bank Teesside A and B Export Cable Corridor

VER	DATE	REMARKS	Drawn	Checked
1	10/12/2012	Draft	FK	DB
2	15/10/2013	Final	LW	DB

DRAWING NUMBER: **9X5889/04/046**

SCALE	1:900,000	PLOT SIZE	A4	DATUM	WGS84	PROJECTION	UTM31N

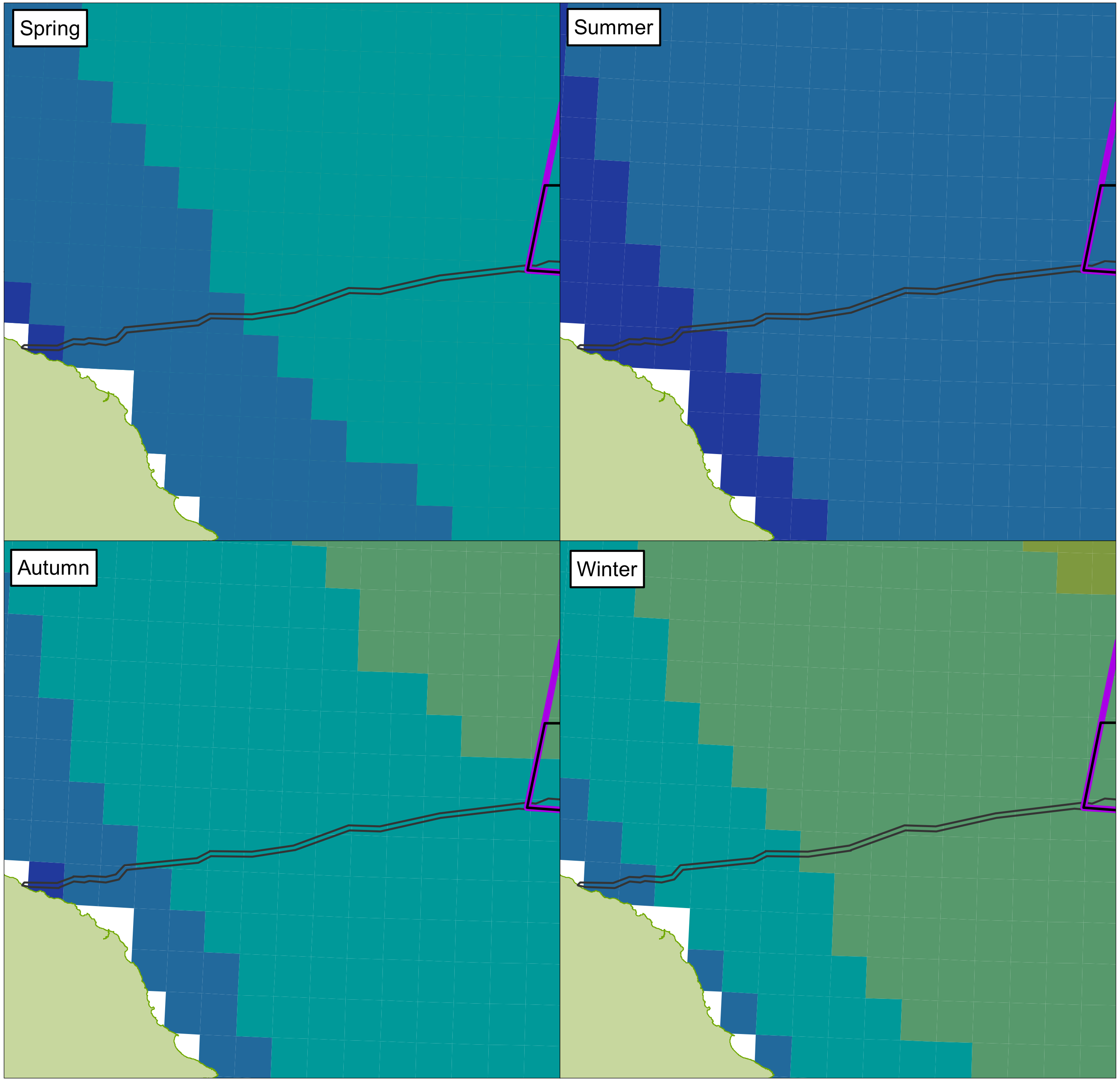

LEGEND

▭ Dogger Bank Zone

▭ Tranche A Boundary

▭ Dogger Bank Teesside A & B Export Cable Corridor

Seasonal Mean Significant Wave Height (m)

■	0.51 - 1.00
■	1.01 - 1.50
■	1.51 - 2.00
■	2.01 - 2.50
■	2.51 - 3.00

Data Source:
BERR (http://www.renewables-atlas.info/)

PROJECT TITLE

DOGGER BANK TEESSIDE A & B

DRAWING TITLE

Figure 3.7 Seasonal Mean Significant Wave Height Across the Dogger Bank Teesside A and B Export Cable Corridor

VER	DATE	REMARKS	Drawn	Checked
1	10/12/2012	Draft	FK	DB
2	15/10/2013	Final	LW	DB

DRAWING NUMBER: **9X5889/04/047**

SCALE	1:1,800,000	PLOT SIZE	A4	DATUM	WGS84	PROJECTION	UTM31N

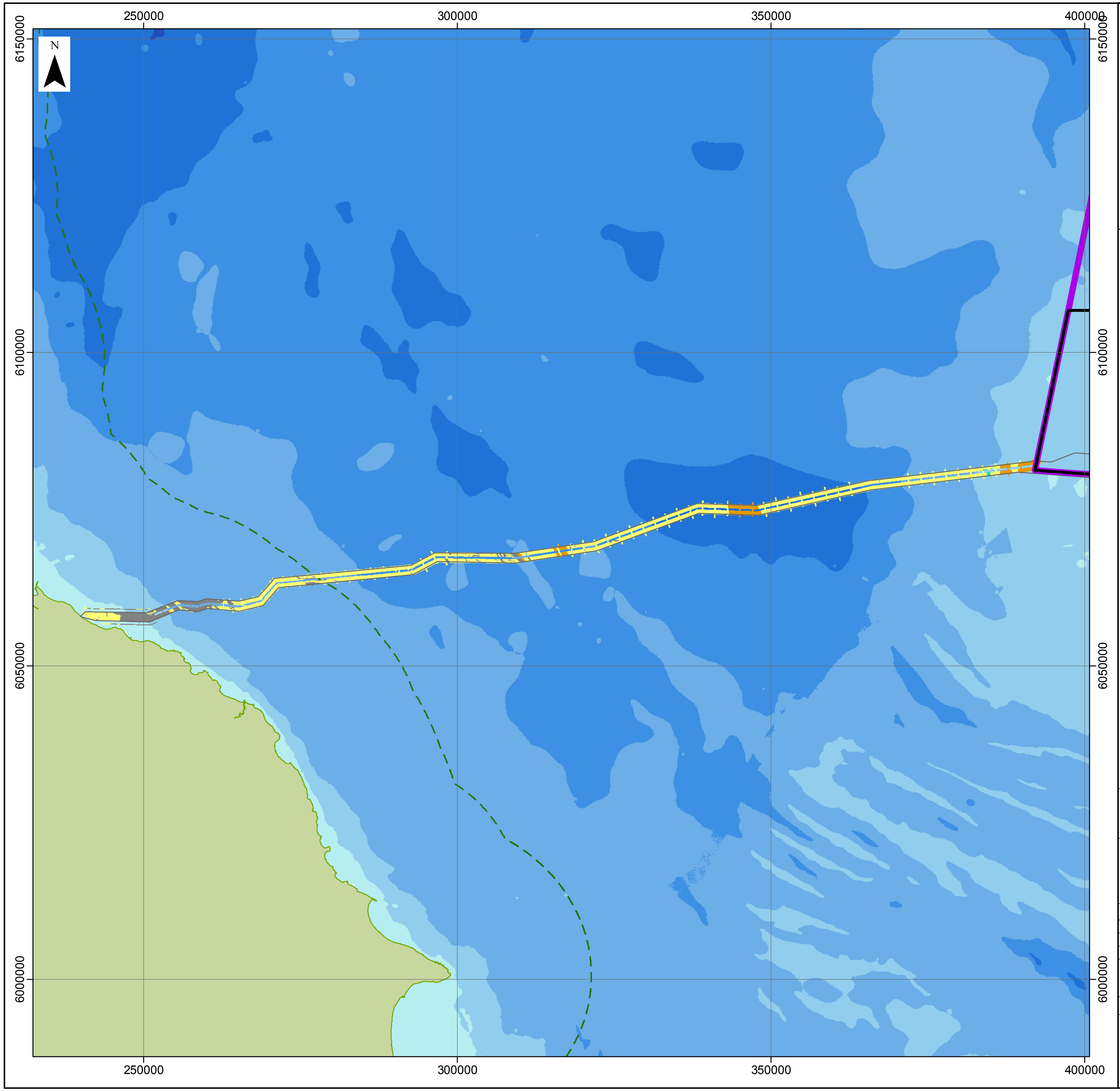

LEGEND

- ▭ Dogger Bank Zone
- ▭ Tranche A Boundary
- ▭ Dogger Bank Teesside A & B Export Cable Corridor
- – – – 12nm Territorial Boundary

Cable Corridor Seabed Sediments

- 🟧 Gravel
- 🟨 Sand
- ⬛ Rock
- 🟩 Till

0 40
Kilometres

Data Source:
Seabed sediments data from Gardline (2012),
Background bathymetry image derived in part from TCarta data © 2009

PROJECT TITLE

DOGGER BANK TEESSIDE A & B

DRAWING TITLE

Figure 3.8 Export Cable Corridor Seabed Sediment Distribution

VER	DATE	REMARKS	Drawn	Checked
1	08/03/2013	Draft	FK	DB
2	15/10/2013	Final	LW	DB

DRAWING NUMBER: **9X5889/04/048**

SCALE	1:910,830	PLOT SIZE	A4	DATUM	WGS84	PROJECTION	UTM 31N

FOREWIND

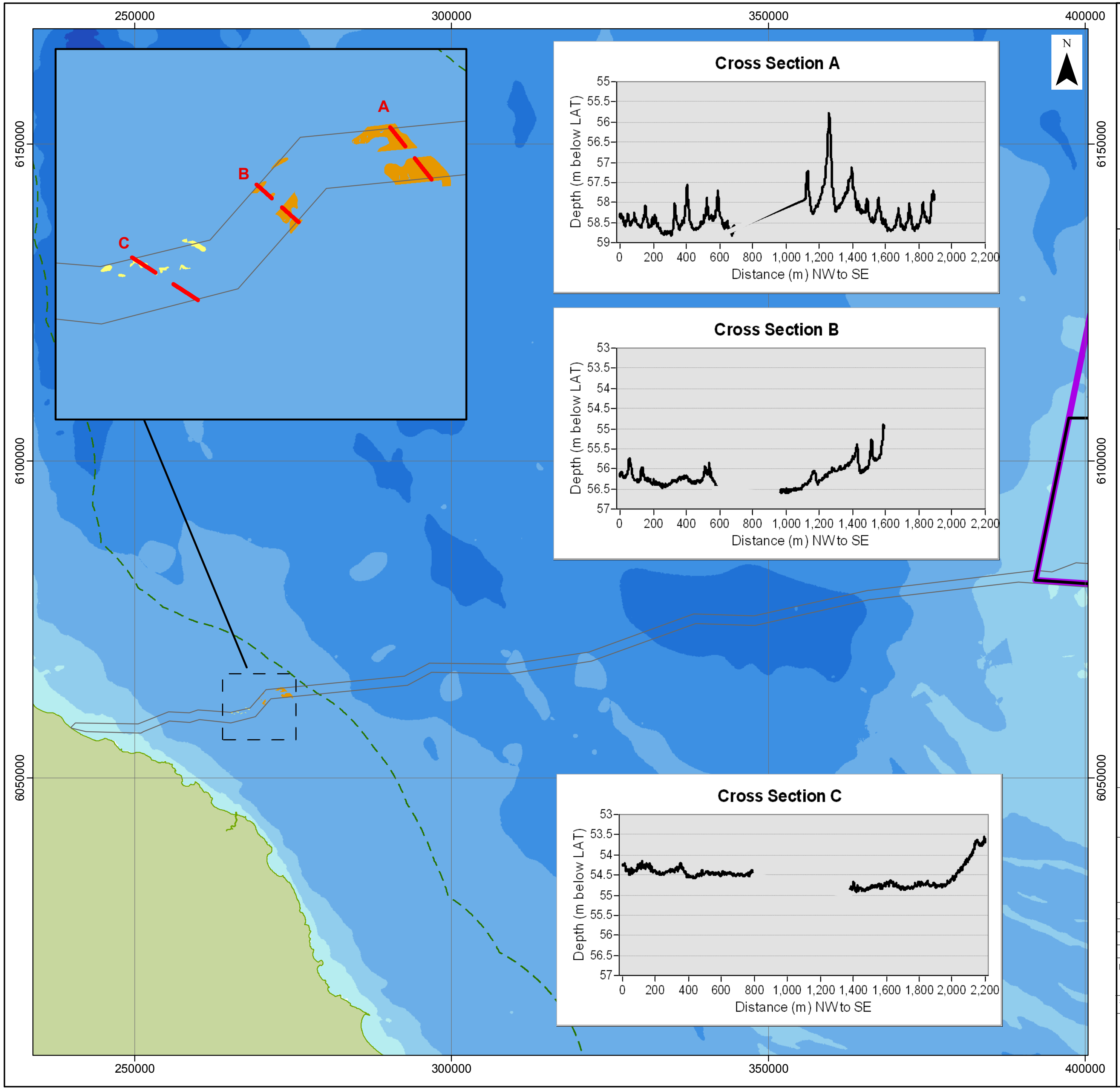

LEGEND

- ▭ Dogger Bank Zone
- ▭ Tranche A Boundary
- ▭ Dogger Bank Teesside A & B Export Cable Corridor
- - - - 12nm Territorial Boundary

Distribution of Megaripples and Sand Waves

- 🟨 Megarippled Sand
- 🟧 Megarippled Sand and Sand Waves
- ━ Cross Section

0 40
Kilometres

Data Source:
Megaripples and Sand Waves data © Gardline, 2012,
Background bathymetry image derived in part from TCarta data © 2009

PROJECT TITLE

DOGGER BANK TEESSIDE A & B

DRAWING TITLE

Figure 3.9 Export Cable Corridor Distribution of Megaripples and Sand Waves

VER	DATE	REMARKS	Drawn	Checked
1	08/03/2013	Draft	FK	DB
2	15/10/2013	Final	LW	DB

DRAWING NUMBER: **9X5889/04/049**

SCALE	1:900,000 / 1:160,000	PLOT SIZE	A4	DATUM	WGS84	PROJECTION	UTM 31N

FOREWIND

APPENDICES

Appendix A: Particle Size Analyses

Particle size distribution of seabed sand samples across the export cable corridor for Dogger Bank Teesside A & B ordered by decreasing percentage of sand. Locations are shown in Figure 1.3.

Sample ID	% sand	% gravel	% mud	D_{50} (mm)	Classification
TCC_GRAB_85	98.7	0.1	1.3	0.19	Slightly Gravelly Sand
TCC_GRAB_84	98.4	0.0	1.5	0.16	Slightly Gravelly Sand
TCC_GRAB_95	98.3	0.1	1.6	0.17	Slightly Gravelly Sand
TCC_GRAB_86	98.3	0.1	1.6	0.15	Slightly Gravelly Sand
TCC_GRAB_93	98.0	0.2	1.8	0.18	Slightly Gravelly Sand
TCC_GRAB_112	97.9	0.0	2.0	0.20	Slightly Gravelly Sand
TCC_GRAB_94	97.7	0.1	2.2	0.17	Slightly Gravelly Sand
TCC_GRAB_100	97.7	0.2	2.1	0.15	Slightly Gravelly Sand
TCC_GRAB_82	97.6	1.0	1.4	0.24	Slightly Gravelly Sand
TCC_GRAB_114	97.6	0.4	2.1	0.17	Slightly Gravelly Sand
TCC_GRAB_90	97.4	0.1	2.5	0.18	Slightly Gravelly Sand
TCC_GRAB_109	97.4	0.0	2.6	0.17	Slightly Gravelly Sand
TCC_GRAB_120	97.3	1.3	1.4	0.16	Slightly Gravelly Sand
TCC_GRAB_92	97.3	0.2	2.5	0.20	Slightly Gravelly Sand
TCC_GRAB_116	97.3	0.4	2.4	0.16	Slightly Gravelly Sand
TCC_GRAB_87	97.2	0.2	2.5	0.19	Slightly Gravelly Sand
TCC_GRAB_79	96.9	1.3	1.8	0.27	Slightly Gravelly Sand
TCC_GRAB_64	96.9	0.3	2.8	0.15	Slightly Gravelly Sand
TCC_GRAB_101	96.8	0.1	3.2	0.15	Slightly Gravelly Sand
TCC_GRAB_102	96.4	0.1	3.4	0.15	Slightly Gravelly Sand
TCC_GRAB_99	96.4	0.5	3.0	0.17	Slightly Gravelly Sand
TCC_GRAB_61	96.4	0.1	3.6	0.15	Slightly Gravelly Sand
TCC_GRAB_62	96.2	0.1	3.7	0.15	Slightly Gravelly Sand
TCC_GRAB_113	96.0	1.0	3.0	0.16	Slightly Gravelly Sand
TCC_GRAB_97	95.9	1.1	3.0	0.18	Slightly Gravelly Sand
TCC_GRAB_103	95.1	0.1	4.8	0.15	Slightly Gravelly Sand
TCC_GRAB_107	95.0	0.1	4.9	0.15	Slightly Gravelly Sand
TCC_GRAB_106	92.6	0.0	7.4	0.15	Slightly Gravelly Sand
TCC_GRAB_78	91.5	7.2	1.2	0.30	Gravelly Sand
TCC_GRAB_111	89.1	8.6	2.3	0.21	Gravelly Sand
TCC_GRAB_118	85.8	12.7	1.5	0.17	Gravelly Sand
TCC_GRAB_80	78.9	19.0	2.1	0.39	Gravelly Sand
TCC_GRAB_71	63.2	16.1	20.7	0.28	Gravelly Muddy Sand

Particle size distribution of gravelly seabed sediment samples across the export cable corridor for Dogger Bank Teesside A & B. Locations are shown in Figure 1.3

Sample ID	% sand	% gravel	% mud	D_{50} (mm)	Classification
TCC_GRAB_75	58.4	31.8	9.8	0.60	Muddy Sandy Gravel
TCC_GRAB_115	34.4	64.8	0.8	5.08	Sandy Gravel
TCC_GRAB_76	33.5	61.5	5.0	20.39	Muddy Sandy Gravel

Appendix C: Dogger Bank Teesside A & B landfall site conceptual model

Conceptual Model – Landfall Dogger Bank Teesside A & B

Forewind

20 January 2014
Final Report
9X5889

HASKONING UK LTD.
WATER

Rightwell House
Bretton
Peterborough PE3 8DW
United Kingdom
+44 1733 334455 Telephone
01733262243 Fax
info@peterborough.royalhaskoning.com E-mail
www.royalhaskoning.com Internet

Document title	Conceptual Model – Landfall Dogger Bank Teesside A & B
Document short title	Conceptual Model - Landfall
Status	Final Report
Date	20 January 2014
Project name	Dogger Bank Teesside Physical Processes
Project number	9X5889
Client	Forewind
Reference	9X5889/R05/303294/Newc

Drafted by	Nick Cooper	
Checked by	David Brew	David S Brew
Date/initials check	20/01/2104	
Approved by	Nick Cooper	
Date/initials approval	20/01/2014	N. J. Cooper

NON TECHNICAL SUMMARY

Forewind Limited is in the process of developing the Dogger Bank Offshore Wind Farm Round 3 Zone. It is proposed that the export cables of four development projects within this Zone will make landfall within two corridors between the seaside towns of Redcar and Marske-by-the-Sea.

This conceptual model provides a baseline understanding of the function and natural characteristics of this section of coastline to provide an appreciation of the likely potential modes of change during construction of the export cable landfalls.

It uses existing data to describe hydrodynamic and wave conditions, sediment transport, morphological change and coastal management (defences and the management policies) along the frontage, especially focusing on the shore in vicinity of the two landfall corridors but set within a broader frontage extending between the River Tees estuary and Saltburn-by-the-Sea, to ensure that potential wider-scale effects on adjacent shores are considered.

Taking account of this conceptual model, the key physical process considered to be affected by construction of the landfalls is sediment transport.

Longshore sediment transport is generally to the southeast within the envelope of the two landfall corridors, but rates are relatively low. This means that whilst ‘downdrift’ frontages may be affected by construction works, the magnitude of change is likely to be low and temporary. However, during storm events, sediment transport from onshore to offshore becomes an important process to consider.

Observed patterns of morphological change along the beaches will also be important considerations in the design of the cable landfalls. Since monitoring began in 2008, short-term variations in beach level of up to ±0.6m have been recorded within the envelope of the two cable landfall corridors.

Future projections of coastal slope erosion are also important design considerations and it is likely that occasional small-scale slumps will occur into the future. Taking future sea-level rise into consideration, the Shoreline Management Plan suggested a long-term erosion rate of 0.4myr^{-1} for these coastal slopes.

CONTENTS

1 INTRODUCTION

1.1 Redcar and Cleveland Coast

1.1.1 Forewind Limited is currently considering the environmental implications of export cable landfalls between the seaside towns of Redcar and Marske-by-the-Sea on the Redcar and Cleveland coast (Figure 1.1), as part of its development of the Dogger Bank Offshore Wind Farm Round 3 Zone. The export cables from four development projects within the Dogger Bank Zone are proposed to make landfall along two corridors within this area before onshore cables connect each to the National Grid. Two projects will connect to the National Grid at the Lackenby substation and two at a site close to Lackenby. Collectively, these four projects are referred to as Dogger Bank Teesside.

1.1.2 This conceptual model provides a baseline understanding of the function and natural characteristics of this section of the Redcar and Cleveland coastline to provide an appreciation of the likely potential modes of change during construction of the export cable landfall. It uses existing data to describe hydrodynamic and wave conditions, sediment transport, morphological change and coastal management (defences and the management policies) along the frontage, specifically in the vicinity of Redcar and Marske-by-the-Sea. Taking account of this conceptual model, the key potential effects on physical and sedimentary processes are then briefly scoped.

1.1.3 The Redcar and Cleveland coastline of principal interest to the assessment of cable landfall effects forms a continuum of sandy beaches (the boundary between each beach is imperceptible) extending between the mouth of the River Tees estuary in the northwest and Saltburn-by-the-Sea in the southeast. The frontage is typically subdivided into Coatham Sands, Redcar Sands, Marske Sands and Saltburn Sands.

1.1.4 Coatham Sands is backed by extensive dunes, Redcar Sands by the town of Redcar which is protected by sea defences, Marske Sands by coastal slopes comprised of glacial till, and Saltburn Sands by steeper cliffs again with sea defences in places (Figure 1.2).

1.2 Shoreline Management Policies

1.2.1 The North East Coastal Authority Group (NECAG) published a Shoreline Management Plan (SMP) in February 2007 (Royal Haskoning, 2007) which outlines the shoreline management policies for this section of the Redcar and Cleveland coastline. Management policies and coastal change tendencies are considered over three different epochs within a SMP spanning the next 100 years. These policies are important as they provide information on the long-term management strategies for this stretch of coastline and their implications for the potential landfall site. Four general policies are considered within the SMP:

- Hold the Line (HTL): this option involves fixing the shoreline position by the provision or maintenance of coastal defences;
- Advance the Line (ATL): this involves building new defences seaward of the original shore, and is usually limited to areas where significant land reclamation is being considered;
- No Active Intervention (NAI): a decision not to invest in providing or maintaining defences; and
- Managed Realignment (MR): allowing the shoreline to move backwards, with management to control/limit the extent of landward retreat.

1.2.2 The SMP policy for the coastline between the South Gare Breakwater at the mouth of the River Tees estuary and Saltburn-by-the-Sea is summarised in Table 1.1, with the locations of distinct SMP management areas shown in Figure 1.3.

Table 1.1. Shoreline Management Plan Policy for the coastline.

SMP Policy Unit	Epoch 1: 2010-2025	Epoch 2: 2025-2055	Epoch 3: 2055-2105	Comments
13.6 South Gare Breakwater	HTL	HTL	HTL	
13.7 Coatham Sands	NAI	NAI	NAI	Detailed flood risk assessment of developed areas.
14.1 Coatham East	HTL	HTL	HTL	Consideration of a transition zone between new defences at Redcar and Coatham Sands
14.2 Redcar	HTL	HTL	HTL	Look to local management to maintain beach
14.3 Redcar East	HTL	HTL	MR	Strategic control
15.1 Red Howles	NAI	NAI	NAI	
15.2 Marske	HTL	HTL	MR	Headland control
15.3 Marske Sands	NAI	NAI	NAI	
15.4 Saltburn	HTL	HTL	HTL	

1.2.3 The two landfall corridors are proposed to be located within the Red Howles Policy Unit of the frontage, where the SMP policy is NAI. Therefore the coastal slopes would be expected to retreat landwards over time in response to coastal erosion.

1.3 Environmental Designations

1.3.1 The frontage within the envelope of the two proposed landfall corridors has no environmental designations. However, it is located close to the Redcar Rocks Site of Special Scientific Interest (SSSI) and Regionally Important Geological and Geomorphological Site (RIGS), and the Teesmouth and Cleveland Coast Special Protection Area (SPA) and Ramsar site (Figure 1.4).

1.4 Structure of this Conceptual Model

1.4.1 This report comprises five sections of which this introduction is Section 1. Section 2 outlines the hydrodynamic processes which characterise this section of the Redcar and Cleveland frontage. Section 3 provides an overview of the sedimentary processes and geomorphological change driven by hydrodynamics, geology and coastal defences present along the frontage. Section 4 briefly scopes the potential effects and sensitivities of the sedimentary processes to changes in the coastal system caused by the landfall. Conclusions are drawn in Section 5.

2 HYDRODYNAMIC PROCESSES

2.1 Predicted Astronomic Tidal Levels

2.1.1 The tidal regime along this section of the Redcar and Cleveland coast is semi-diurnal; the water level rises and falls twice a day. The tide levels at the landfall location will be similar to those provided in the 2013 Admiralty Tide Tables for the River Tees (Table 2.1).

Table 2.1. Tidal levels at River Tees (from the 2013 Admiralty Tide Tables).

Datum	m LAT	m ODN
Highest Astronomical Tide	6.1	3.25
Mean High Water Spring	5.5	2.65
Mean High Water Neap	4.3	1.45
Mean Sea Level	3.2	0.35
Mean Low Water Neap	2.0	-0.85
Mean Low Water Spring	0.9	-1.95
Lowest Astronomical Tide	0.0	-2.85

Note: Ordnance Datum Newlyn (ODN) is 2.85m above Lowest Astronomical Tide (LAT).

2.1.2 Table 2.1 shows that the tidal range, the difference between high and low water level, is 4.6m on a spring tide and 2.3m on a neap tide. These are astronomical levels and do not account for meteorological surges.

2.2 Storm Surge and Extreme Water Levels

2.2.1 Water levels on the east coast are strongly influenced by tidal surges, which are driven by low pressure weather systems moving down the North Sea. These have the effect of raising extreme water surfaces above levels that would be caused by astronomical effects alone. The resulting water levels have been quantified, for different return periods, in the Shoreline Management Plan (Royal Haskoning, 2007), and the results for the frontage are shown in Table 2.2. The 200-year extreme water level is 3.87m ODN; an increase above the predicted astronomical spring tide level of about 1.22m.

Table 2.2. Extreme water levels at River Tees (Royal Haskoning, 2007).

Return Period (years)	Water Level (m ODN)
1	3.20
10	3.48
25	3.61
50	3.68
100	3.80
200	3.87

2.3 Relative Sea-level Rise

2.3.1 Sea level rise is controlled by three principal processes; thermal expansion, melting of glaciers and changes in the volume of the ice caps of Antarctica and Greenland. These processes result in an absolute change in sea level that operates at a global scale. In addition, changes in the level of the land mass can have a local effect superimposed upon, or counteracting the absolute global sea level changes. When considering both processes, the term relative sea-level change is used to reflect changes in the level of the sea relative to the level of the local land mass.

Historic Sea-level Rise

2.3.2 Shennan and Horton (2002) compiled data regarding the relative rate of land level uplift around the UK based on radiocarbon dated sea level index points covering the late Holocene (the past 4,000 years). Their best estimate of land level uplift for the River Tees estuary was 0.17mmyr^{-1}, indicating that the River Tees lies very close to the axis of tilt of the land mass in Great Britain. Here, global sea level rise will have a slightly more marked effect than it would do in more northern parts of the UK where rates of land uplift are higher.

2.3.3 Woodworth *et al.* (2002) undertook an analysis of measured tide gauge data for UK sites with more than 15 years data record. The gauge at North Shields provides the longest available record of historic sea levels at a location relatively close to the envelope of the two cable landfall corridors. Between the years 1901 and 1996, relative sea level rise was measure to be 1.86mmyr^{-1}.

Predicted Future Sea-level Rise

2.3.4 Although it is likely that sea-level rise will accelerate into the future, the rates of change are uncertain. Due to this, the United Kingdom Climate Projections launched in 2009 (UKCP09) adopted a probabilistic approach to future sea level projections, based upon three different greenhouse gas emissions scenarios; low, medium and high.

2.3.5 For a grid cell centred on Redcar and Marske-by-the-Sea, UKCP09 projected a 0.20m rise in sea level by 2050 ($50^{\%ile}$ 'most likely' value under the medium greenhouse gas emissions scenario) (Figure 2.1). For the longer term, UKCP09 provides lower and upper bounds projections by 2100 of between 0.18m ($5^{\%ile}$ value, low emissions) and 0.86m ($95^{\%ile}$ value, high emissions) respectively.

2.4 Wave Climate

2.4.1 The predominant offshore wave direction in this sector of the North Sea is from the north, with waves from the northeast also occurring relatively frequently. The highest offshore waves also approach from these directions (Figure 2.2a).

2.4.2 As offshore waves propagate towards the shore, they are influenced by the seabed and shoreline features and so wave transformation processes occur, resulting in a nearshore wave climate. Generally, nearshore waves approach the shore from the north-northeast and northeast due to these transformation processes. There can be notable differences in the nearshore wave heights recorded between summer and winter months.

2.4.3 Storm events from different sectors can also occur, albeit less frequently. During the winter of 1995/96 a prolonged period of easterlies occurred (Figure 2.2b) which was atypical of the general wave climate. This series of storm events caused a significant volume of beach sediment to be removed from the Redcar town beaches and be transported towards the west, along Coatham Sands and into the navigation channel of the River Tees estuary where increased navigation dredging was required as a consequence.

2.5 Tidal Currents

2.5.1 Tidal cycles generate currents of water along the coast as they flood (rise) and ebb (fall). The flood and ebb currents are often different in magnitude, so that there is a net (residual) current. These may be important in driving a net movement of sediment in a particular direction. As the flood tide has slightly stronger currents than the ebb tide, the residual current generally is to the southeast in the vicinity of the envelope of the landfall of the two export cable corridors.

The flood current along the Redcar and Cleveland coastline generally is to the south, running parallel to the coast, but the presence of the River Tees estuary, various maritime structures, headlands and outcrops do locally affect the broader patterns. For example, a localised gyre exists immediately east of the South Gare Breakwater on the flooding tide which has the potential to move sediment transported in suspension in the water column westwards, back towards the mouth of the River Tees estuary.

3 SEDIMENTARY PROCESSES AND BEACH MORPHOLOGICAL CHANGE

3.1 Geology and Coastal Defences

3.1.1 The coastline of principal interest extends between the mouth of the River Tees estuary in the northwest and Saltburn-by-the-Sea in the southeast (Figure 3.1). The frontage is typically subdivided into Coatham Sands, Redcar Sands, Marske Sands and Saltburn Sands.

3.1.2 Coatham Sands extends between the South Gare Breakwater at the mouth of the River Tees estuary and Coatham (Figure 3.2). It is backed by extensive sand dunes which protect Teesside Steel Works against flooding by the North Sea. At their eastern limit the dunes form Cleveland Golf Club. There is a series of slag banks called the German Charlies in the nearshore zone along the western end of Coatham Sands which, together with the South Gare Breakwater, protect the frontage against direct wave attack which has helped to build up the extensive dune system.

3.1.3 Redcar Sands is located in front of the seaside town of Redcar and extends initially along The Esplanade and then further southeast along The Stray (Figure 3.3). It is characterised by a series of rock outcrops in the nearshore zone, collectively called the Coatham and Redcar Rocks. The Environment Agency and Redcar and Cleveland Borough Council are currently jointly working on the construction of a major new sea defence scheme along the Redcar frontage. There has been a long history of catastrophic sea flooding events in the town and the defences are primarily intended to reduce this risk from wave overtopping, whilst also incorporating enhancements to assist with economic regeneration.

3.1.4 Marske Sands extends from Redcar to Saltburn and fronts the smaller seaside town of Marske-by-the-Sea (Figure 3.4). Generally, the shore is backed by undefended and initially low, vegetated till cliffs rising to the higher coastal slopes at Marske-by-the-Sea. The backshore and toe of the coastal slope is composed of a high, dry sandy backshore. Along some there are substantial shingle berms present at the toe of the slopes.

3.1.5 Saltburn Sands is characterised by its seawall, promenade and iconic pier. The frontage is backed by steep cliffs and the small seaside town of Saltburn-by-the-Sea and bounded at its eastern end by Saltburn Scar, a large rock outcrop extending across the intertidal zone and marking a change in coastal alignment as Warsett Hill protrudes into the sea (Figure 3.5). The shoreline is intercepted by the outflow channel of Skelton Beck, which discharges into the North Sea across the sands.

3.1.6 The geological layers of interest for the construction of the Dogger Bank Teesside Projects export cable landfall are:

- till slopes between Redcar and Marske-by-the-Sea;
- sand beaches that front the slopes; and

- occasional outcrops of underlying bedrock and patches of shingle berms at the toe of the slopes.

3.2 Sediment Sources, Transport and Sinks

3.2.1 The Shoreline Management Plan (Royal Haskoning, 2007) provides information on the sources, transport and sinks of sediments along this section of the Redcar and Cleveland coastline by splitting the frontage into three units, discussed below.

South Gare Breakwater to the west end of Coatham Rocks

3.2.2 This stretch of coast is undefended and comprises a 300m wide sand beach (Coatham Sands) backed by low sand dunes forming links (British Geological Survey, 1998). The hinterland comprises a low-lying land-claimed coastal plain (Coatham Marsh) in the mouth of the River Tees estuary and till further southeast towards Redcar. The South Gare Breakwater in the northwest and Coatham Rocks in the southeast hold the beach in place. In addition, the German Charlies slag banks provide further shelter to the coast. The crenulated nature of the bay indicates that the beach plan shape is tending towards an equilibrium form. Sediment is likely to be supplied to the beach from the dunes and from sources offshore in Tees Bay. Indeed, Motyka (1986) suggested that very little beach sediment moves south out of Hartlepool Bay and Tees Bay, which tend to act as sediment traps.

3.2.3 The coastline in this area has been altered considerably by the construction of the North and South Gare Breakwaters. Using map data, Motyka and Beven (1986) determined accretion rates of 130,000m^3/yr north of the River Tees estuary mouth (Seaton Sands) and 107,000m^3/yr to the south (Coatham Sands) between 1891 and 1930. This major accretion occurred as a result of accumulation of sediment against the northern breakwater due to dominant southerly sediment transport, and accumulation to the southeast due to the sheltering effect of the southern breakwater which induces a local reversal of transport in its lee (Babtie, 1997). Motyka and Beven (1986) estimated that the breakwaters have resulted in a reduction of southerly longshore transport by as much as an order of magnitude, to a residual value of around 50,000m^3/yr. Although South Gare Breakwater restricts passage of sediment across the mouth of the River Tees estuary into Coatham Sands, Coatham Rocks appear to be ‘leaky’ and allows sediment to bypass further to the south.

3.2.4 The long-term (1858-1990) historical development of the dunes has been stability (0myr^{-1}), whereas the mean high water and mean low water marks have accreted (1.55myr^{-1} and 0.11myr^{-1}, respectively) (Babtie, 1999). Despite the long-term stability of the dunes, Babtie (1999) concluded that the typical erosion rate for undefended land is 0.1myr^{-1}. The morphology of the dunes suggests that erosion is taking place towards Coatham, whereas they become gradually more stable towards the north.

3.2.5 There are several anthropogenic activities that are influencing sediment budgets along Coatham Sands. Motyka and Beven (1986) suggested that dredging in the mouth of the River Tees estuary is intercepting much of the southerly moving sediment. The role of the River Tees in supplying fine sediment to the coastal zone has been reduced considerably by the construction of the Tees Barrage. The Barrage was designed to allow bypassing of sediment, but observed accumulations upstream, and a 24% reduction in the dredging requirement of the harbour indicates that much of the river sediment is trapped.

3.2.6 In summary, the Coatham Sands beach is held in place by control points at South Gare Breakwater and ‘leaky’ Coatham Rocks. The crenulate shape of the bay between these two points indicates that the beach plan shape is tending towards an equilibrium form.

Redcar Sands

3.2.7 The coastline fronting Redcar headland comprises a sand beach (Redcar Sands) backed by a sea wall and revetments. Seaward of the beach is a well-defined rock shore platform (Coatham and Redcar Rocks) composed of Redcar Mudstone Formation (British Geological Survey, 1998) which controls the position of the headland.

3.2.8 The beach appears to be fairly volatile and sensitive to wave conditions with loss over short periods (e.g. individual storm events or whole winter seasons) followed by recovery over periods of a few years (Babtie, 1997). For example, substantial amounts of sand were lost from this beach during storms in 1995/1996 followed by recovery in 1997. Longshore sediment transport around the headland is to the south (Babtie, 1997, 1999). However, large volumes of sediment could potentially be moved north under easterly storm conditions such as those in winter 1995/96. The mean high water and mean low water marks have suffered long-term (1858-1990) erosion of 0.3 myr^{-1} and 0.17 myr^{-1}, respectively (Babtie, 1999). It is possible that the long-term lowering of Redcar Sands is related to sediment trapping in Tees Bay by North and South Gare Breakwaters.

3.2.9 Redcar headland is a fixed hard point comprising a sea wall and a wide rock shore platform. The presence of a sandy beach fronting the shoreline here indicates that this headland is not a longshore sediment transport barrier and there is connectivity between the beaches to its west (Coatham Sands) and east (Marske Sands).

3.2.10 Beach elevation data shows that the upper 130m of the beach along the western side of the headland slopes gradually seaward from an elevation of 3.4m ODN at the base of the sea wall to around 0.9m ODN at a distance of 130m. The eastern side of the headland, closer to Redcar Rocks, slopes from 1.8m ODN to -0.7m ODN. The data shows a lowering (and likely thinning) of the beach in an easterly direction towards the exposure of shore platform, which is at an average elevation of around 0.7m ODN.

3.2.11 In summary, Redcar 'headland' is a fixed hard point comprising a sea wall and a wide rock shore platform. Although the geomorphological feature is a headland it is fronted by a wide sand beach indicating that it is not a longshore sediment transport barrier and there is connectivity between west and east. From a coastal defence perspective, the sea wall at Coatham Rocks is sensitive, because it is at risk of overtopping with the potential to flood parts of Redcar immediately behind it.

3.2.12 Redcar headland is sensitive to coastal processes because of the unequal distribution of wave energy along this stretch of coast caused by bathymetry variations between Coatham Sands, Redcar Sands and Marske/Saltburn Sands. The changes in water depth result in a low wave energy environment providing sheltered water in the bays (the Sands) and a higher energy environment at the headland (Coatham Rocks and sea wall). This causes increased pressure on the headland relative to the bays to either side.

East end of Coatham Rocks to Saltburn-by-the-Sea

3.2.13 This stretch of coast comprises a wide (300-400m) sand beach (Marske/Saltburn Sands) held in place by Saltburn Scar (a headland composed of Redcar Mudstone Formation) to the east. Along its western end the beach is backed by a rock revetment built on to the face of a narrow strip of sand dune fronting a till hinterland (British Geological Survey, 1998). Here the beach is controlled by groynes, which were nourished with 70m^3 of sand and shingle per metre of frontage between 1973 and 1983. The eastern half is mainly undefended and the beach is backed by a narrow strip of dunes in front of till slopes, apart from a stretch of sea wall in front of Saltburn-by-the-Sea at the eastern extremity. Prior to defences, the dunes and till cliffs appear to have been eroding at a fairly constant rate to form a gently curving bay between Redcar Rocks and Saltburn Scar.

3.2.14 The dunes are in poor health and are actively eroding, forming a 'veneer' in front of the till hinterland. In places, the dunes are absent and till is exposed at the coast. In front of the till, the beach is composite with pebbles forming an upper storm beach with a wide sandy lower beach. This structure indicates that the pebbles are supplied locally through erosion of the till. In front of the dunes, the upper pebble beach breaks down and there are patches of shingle sometimes shaped into cusps on the beach surface, which is mainly sand.

3.2.15 Net longshore sediment transport is to the east (Babtie, 1997, 1999). Numerical modelling suggests that the potential to transport sediment increases gradually from Coatham Sands, across Coatham/Redcar Rocks to Marske Sands. This is probably due to a subtle change in orientation of the coast relative to the predominant wave direction. These differential potential transport rates suggest that more sediment is being lost from Marske/Saltburn Sands than is being delivered from the west, around Redcar headland. Only small sediment build-up on the west side of the Redcar groynes indicates that actual longshore sediment transport is low in this area. In addition, the presence of Saltburn Scar does not allow much loss of sediment to the east.

3.2.16 Babtie (1999) showed that over the long-term (1858-1990), the mean high water mark has consistently retreated (0.04-0.74myr^{-1}, with the highest values in the west). The mean low water mark has also retreated in most areas (0.15-0.8myr^{-1}) but with local accretion at Marske-by-the-Sea (0.01myr^{-1}). Overall, Babtie (1999) estimated the erosion rate for undefended land to be around 0.4myr^{-1} with localised rates of 0.6-0.7myr^{-1} closer to Redcar.

3.2.17 In summary, Marske/Saltburn Sands is held in place by a control point at Saltburn-by-the-Sea (Saltburn Scar). Prior to construction of defences, the dunes and till cliffs appear to have been eroding at a fairly constant rate, to form a gently curving bay between Coatham Rocks and Saltburn Scar. However, the crenulate shape of the bay is now interrupted by the presence of a revetment and groynes (in its western half). The revetment forms a hard stretch which has caused the bay to protrude slightly seaward of its ‘natural’ shape, and the wall is therefore a pressure point. The sea wall at Saltburn-by-the-Sea is sensitive to overtopping.

3.3 Suspended Sediment Transport

3.3.1 Numerical modelling undertaken to inform the Environmental Statement for the Northern Gateway Container Terminal (Royal Haskoning, 2006) identified the importance of wave-stirring of the seabed sediments in inducing sediment mobilisation as tidal currents alone are relatively weak. There is, however, relatively little quantitative information on existing (baseline) suspended sediment concentrations along the frontage.

3.4 Beach Morphological Change

3.4.1 Since 2008, Redcar and Cleveland Borough Council has been monitoring beach morphological change as part of the wider Cell 1 (North East) Regional Coastal Monitoring Programme (Cooper *et al.*, 2009). This has included:

- six-monthly beach profile surveys at nine transects between Coatham Sands and Saltburn Sands;

- six-monthly or annual beach topographic surveys along Coatham Sands, Redcar Sands, Marske Sands and Saltburn Sands;
- walk-over inspections of the coastal defences, cliffs, dunes and beaches every two years; and
- a single bathymetric and geophysical survey transect extending from Saltburn offshore to the 20m seabed contour, including seabed grab samples at 1km intervals along the transect.

3.4.2 Analysis of the data shows that patterns of both longshore transport of beach sediment and onshore-offshore transport during storm events are important. Generally, sediment is transported at relatively slow rates towards the southeast along the shore. Waves predominantly approach the shore from the north, north-northeast and northeast, so longshore sediment transport rates are small as the waves are relatively normal to the shore. However, during rougher winter conditions, beach sediment can be drawn down into the nearshore zone, where it is transported longshore towards the southeast by tidal currents, before returning to the beach during calmer conditions.

3.4.3 Occasionally, storms from south easterly and easterly directions can transport sand westwards along the Redcar and Coatham Sands, towards the River Tees estuary. Such a succession of events occurred in 1995/96, causing much (temporary) sand loss from Redcar Sands and extensive sand deposition within the navigation channel of the River Tees estuary which required maintenance dredging to ensure continued safe navigation passage to vessels.

3.4.4 Since 2008, the monitoring results have shown that different parts of the frontage are subject to different responses, with sediment being moved around the foreshore quite extensively. However, overall, there has been a net accretion of sand along the entire frontage between Coatham Sands and Saltburn Sands over this time.

3.4.5 Beach profile RC7 is located within the envelope of the two cable landfall corridors. Figure 3.6 shows the variations in beach and coastal slope profile over time between November 2008 and April 2011. The profiles describe changes to foreshore levels of up to 0.6m over this short period.

3.5 Saltburn Bathymetric Transect

3.5.1 At Saltburn-by-the-Sea, a bathymetric survey was surveyed in 2010 as part of the Cell 1 (North East) Regional Coastal Monitoring Programme. This bathymetric transect extends 4km offshore, where the seabed reaches a depth of -25m ODN. BGS data shows the area is underlain by Jurassic limestone and mudstone of the Lias Group. Seabed mapping and a characteristic profile drawn through the data show the seabed can be separated into two zones:

- a nearshore zone that extends to 2.5km from the coast to 20m depth, which is sandy and smooth, with a mean gradient of 0.4^{o}.

This zone is generally featureless, with occasional small outcrops of rock and no bedforms can be discerned. The seabed samples in this zone show fine sand, while BGS seabed sediment mapping shows gravelly muddy sand in the nearshore area becoming slightly gravelly muddy sand further offshore.

- an offshore zone that extends from 2.5km to 4km offshore, characterised by a rugged seabed with a mean gradient of 0.1^{o}. Bedrock crops out throughout the zone with clear evidence for gently dipping strata with a strike of east-northeast to west-southwest. The outcrop shows forms ranging from distinct saw-toothed dip and scarp slopes to isolated bedrock ‘reefs’ with *in situ* rock and detached boulders. This variation probably reflects changes in rock strength. Seabed sediments in this zone are located in bedrock hollows and samples range from very coarse sand to very fine sand. BGS seabed sediment mapping shows slightly gravelly muddy sand throughout the area, and does not recognise any bedrock outcrop. This difference probably reflects the low resolution of the BGS data.

4 POTENTIAL EFFECTS OF LANDFALL

4.1 Potential Effects during Construction

4.1.1 This section focuses upon those elements of the construction phase that would have the greatest potential to affect physical and sediment transport processes at the landfall site. These include beach work activities to install the cable that may cause the following coastal process impacts:

- changes to the sediment transport processes within the envelope of the two landfall corridors due to the effects of trenching and cable laying across the shore and nearshore zone; and
- disturbance of the ‘down-drift’ sediment transport necessary for the continued supply of sand towards Saltburn-by-the-Sea.

4.2 Potential Effects during Operation

4.2.1 There are anticipated to be no effects during the operation of the landfall site because the cables will buried beneath the beach and coastal slope. However, potential effects to sediment transport may arise if mattressing or rock armouring is used in the nearshore zone.

4.3 Potential Effects during Decommissioning

4.3.1 The effects during decommissioning will be similar to those described during the construction phase.

5 CONCLUSIONS

5.1.1 The conclusions regarding baseline conditions outlined below are selected based on how sensitive the particular parameter is to changes at the landfall site. In the case of this section of the Redcar and Cleveland coast, the baseline parameter that is most likely to be affected by construction of the landfall is sediment transport. The observed patterns of beach morphological change will also be important in the design of the cable landfall.

5.1.2 **Sediment Transport**: Longshore sediment transport is generally to the southeast along most of this section of the Redcar and Cleveland coast, including within the envelope of the two landfall corridors, although transport reversals occur in the vicinity of the South Gare Breakwater. Rates of sediment transport longshore are relatively low, but onshore to offshore transport does occur in quite significant volumes during storm events.

5.1.3 **Beach and Slope Morphological Change**: Whilst sand beaches extend continuously along Coatham Sands, Redcar Sands, Markse Sands and Saltburn Sands, there is rarely a uniform beach response along this whole section. Instead, it appears that sand gets moved between beaches quite readily and during storm events is drawn-down the profile to the nearshore zone, where it may become entrained by tidal currents and swept towards the southeast. Since monitoring began in 2008, changes in beach level of up to 0.6m have been recorded in the vicinity of the envelope of the two cable landfall corridors. The backing coastal slopes in this area are expected to exhibit recession through occasional small-scale slumping and a long-term erosion rate of 0.4myr^{-1} has been projected in the SMP, accounting for likely increases in future sea-level rise.

6 REFERENCES

Babtie. 1999. Seaham Harbour to Saltburn Shoreline Management Plan. Report to Easington District Council, Hartlepool Borough Council and Redcar & Cleveland Borough Council. March 1999.

Babtie. 1997. Redcar Beach Study. Report to Redcar & Cleveland Borough Council. August 1997.

British Geological Survey. 1998. Guisborough. Sheet 34. Solid and Drift Geology.

Cooper, N.J., Rowe, S., Parsons, A. and Cooper, T. 2009. Cell 1 Regional Coastal Monitoring Programme. Proceedings Flood and Erosion Risk Management Conference, Telford.

Motyka, J.M. 1986. A Macro Review of the Coastline of England and Wales. Volume 2 – The East Coast (The Tees to The Wash). HR Wallingford Report SR107.

Motyka, J.M. and Bevan, S.M. 1986. A Macro Review of the Coastline of England and Wales. Volume 1 – The North East Coast (St Abb’s Head top the Tees). HR Wallingford Report SR90.

Royal Haskoning. 2007. River Tyne to Flamborough Head Shoreline Management Plan 2. Report to North East Coastal Authorities Group (NECAG), February 2007.

Royal Haskoning. 2006. Northern Gateway Container Terminal Environmental Statement. Report produced for PD Teessport, April 2006.

Shennan, I. and Horton, B. 2002. Holocene land- and sea-level changes in Great Britain. Journal of Quaternary Science, 17, 511–526.

Woodworth, P.L., Le Provost, C., Rickards, L.J., Mitchum, G.T. and Merrifield, M. 2002. A review of sea-level research from tide gauges during the World Ocean Circulation Experiment. In: Oceanography and marine biology: an annual review. Gibson, RN, Barnes M and Atkinson RJA, Eds. London: Taylor & Francis, 40.

UKCP09. Available from: http://ukclimateprojections.defra.gov.uk/

7 GLOSSARY

7.1.1 Table 7.1 provides a glossary of terms and abbreviations used in this conceptual model.

Table 7.1. Glossary of terms and abbreviations used in this conceptual model.

ATL	Advance the Line
NECAG	North East Coastal Authority Group
HTL	Hold the Line
LAT	Lowest Astronomical Tide
MR	Managed Realignment
NAI	No Active Intervention
ODN	Ordnance Datum Newlyn
RIGS	Regionally Important Geological and Geomorphological Sites
SAC	Special Area of Conservation
SMP	Shoreline Management Plan
SPA	Special Protection Area
SSSI	Site of Special Scientific Interest
UKCP09	United Kingdom Climate Projections 2009

FIGURES

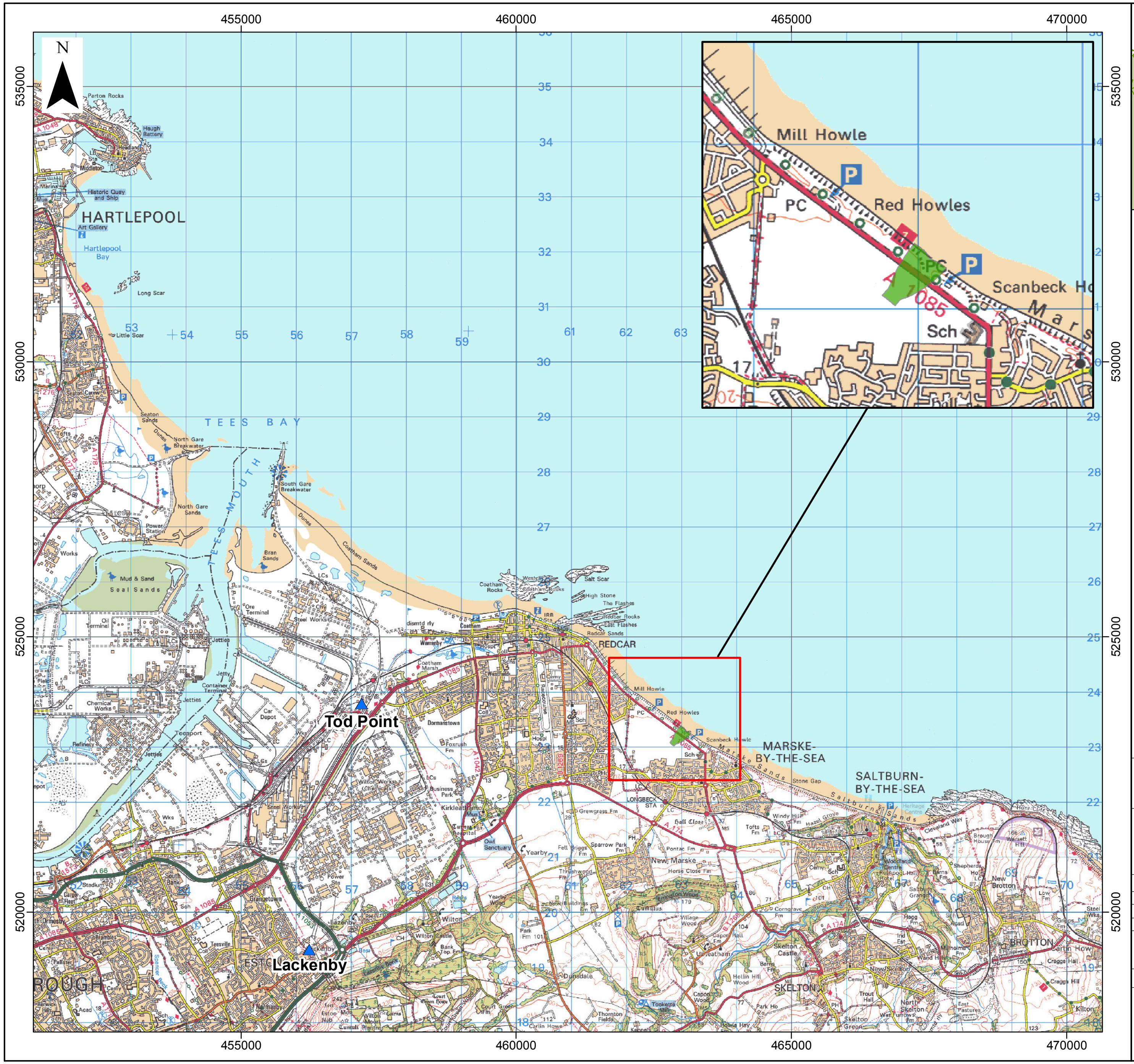

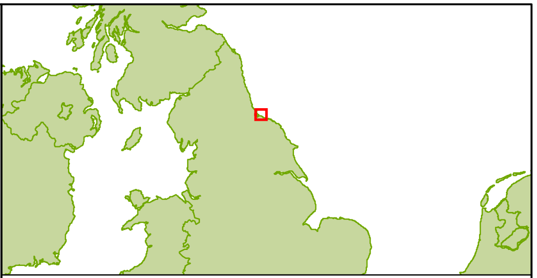

LEGEND

🟩 Dogger Bank Teesside A & B Cable Landfall Envelope

▲ National Grid Substations

0 3
Kilometres

Source:
Substations © National Grid, 2010,
Ordnance Survey © Crown copyright
All rights reserved. 2012 Licence number 0100031673

PROJECT TITLE

DOGGER BANK TEESSIDE

DRAWING TITLE

Figure 1.1 Location Plan

VER	DATE	REMARKS	Drawn	Checked
1	04/12/2012	Draft	FK	NC
2	15/10/2013	Final	LW	NC

DRAWING NUMBER: **9X5889/01**

SCALE	1:105,000	PLOT SIZE	A4	DATUM	OSGB36	PROJECTION	BNG

FOREWIND

A - Coatham Sands - Sand Beach and Dunes at Coatham Sands (Note: Redcar Steel Works visible on the backing lad)

B - Redcar Sands - Sand Beach and Sea Defences fronting Redcar Town (Note: Sea defences are currently being replaced as part of a capital scheme)

C - Marske Sands - Sand Beach with Narrow Shingle Berm and backed by Till Slopes (Note: The coastal slopes are initially low but rise with south-easterly progression along the frontage)

D - Saltburn Sands - Sand Beach with Narrow Shingle Berm and backed by Seawall, Promenade and Steep Sea Cliffs (Note: Iconic Saltburn Pier on foreshore)

Source:

PROJECT TITLE

DOGGER BANK TEESSIDE

DRAWING TITLE

Figure 1.2 Coastal Characteristics

VER	DATE	REMARKS	Drawn	Checked
1	04/12/2012	Draft	FK	NC
2	08/01/2013	Final	FK	NC

DRAWING NUMBER: **9X5889/02**

SCALE	PLOT SIZE	DATUM	PROJECTION
Not to scale	A4		

FOREWIND

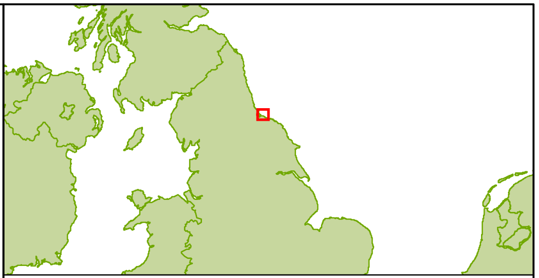

LEGEND

🟩 Dogger Bank Teesside A & B Cable Landfall Envelope

▬ Policy Unit*

*Policy Unit

13.6 = South Gare Breakwater
13.7 = Coatham Sands
14.1 = Coatham East
14.2 = Redcar
14.3 = Redcar East
15.1 = Red Howles
15.2 = Marske
15.3 = Marske Sands
15.4 = Saltburn

0 3
Kilometres

Source:
River Tyne to Flamborough Head Shoreline Management Plan 2.
Ordnance Survey © Crown copyright
All rights reserved. 2012 Licence number 0100031673

PROJECT TITLE

DOGGER BANK TEESSIDE

DRAWING TITLE

Figure 1.3 Shoreline Management Plan 'Policy Units'

VER	DATE	REMARKS	Drawn	Checked
1	04/12/2012	Draft	FK	NC
2	15/10/2013	Final	FK	NC

DRAWING NUMBER: **9X5889/03**

SCALE	1:105,000	PLOT SIZE	A4	DATUM	OSGB36	PROJECTION	BNG

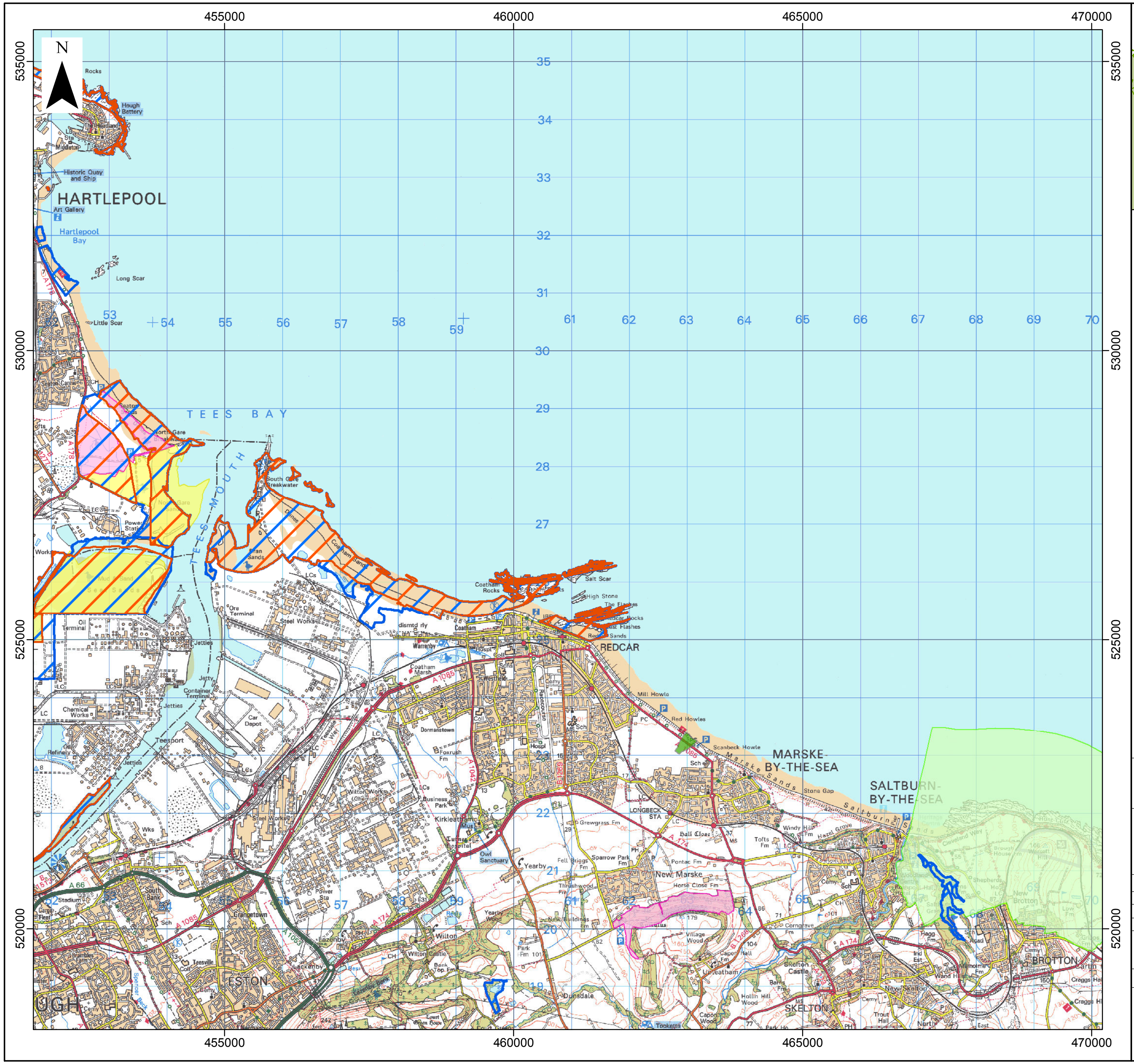

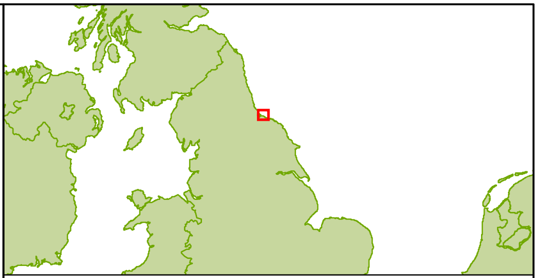

LEGEND

- 🟩 Dogger Bank Teesside A & B Cable Landfall Envelope
- ▨ Site of Special Scientific Interest (SSSI)
- ▨ SPA/Ramsar
- 🟪 Local Nature Reserve (LNR)
- 🟨 National Nature Reserve (NNR)
- 🟩 Heritage Coast

0 3
Kilometres

Source:
Natural England
Ordnance Survey © Crown copyright
All rights reserved. 2012 Licence number 0100031673

PROJECT TITLE

DOGGER BANK TEESSIDE

DRAWING TITLE

Figure 1.4 Environmental Designations

VER	DATE	REMARKS	Drawn	Checked
1	04/12/2012	Draft	FK	NC
2	15/10/2013	Final	LW	NC

DRAWING NUMBER: 9X5889/04

SCALE	1:100,000	PLOT SIZE	A4	DATUM	OSGB36	PROJECTION	BNG

FOREWIND

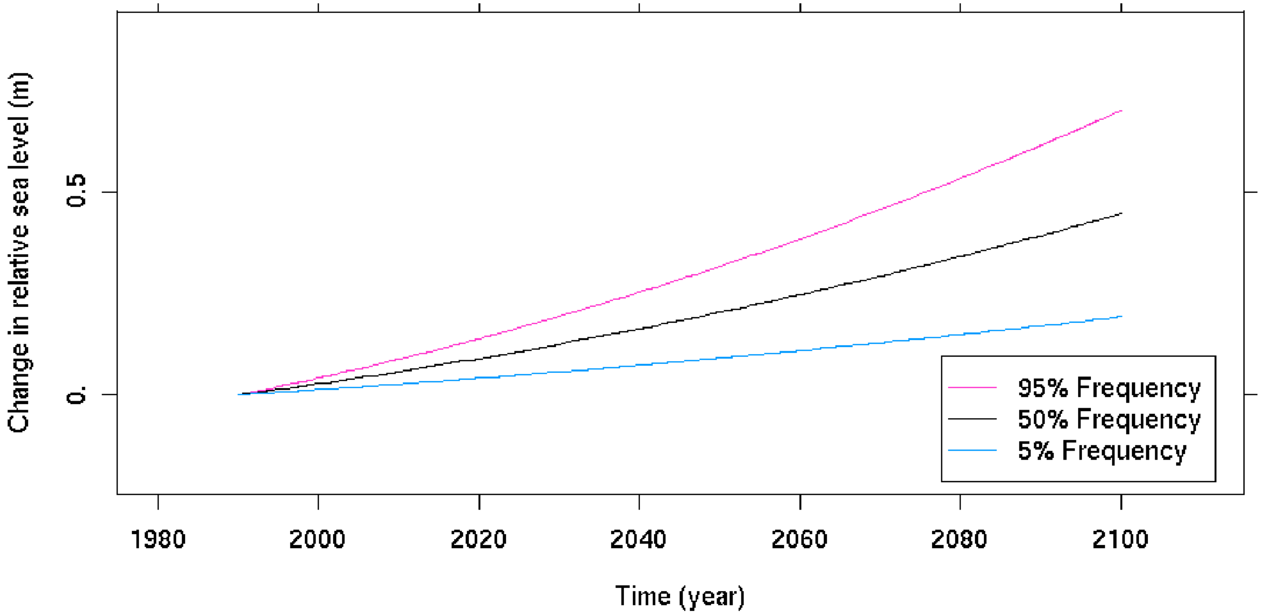

Source:
United Kingdom Climate Projections 2009 (UKCP09)

PROJECT TITLE	*DOGGER BANK TEESSIDE*
DRAWING TITLE	**Figure 2.1 Future Sea Level Rise Projections at Redcar and Marske-by-the-Sea (UKCP09 Medium Emission Scenario)**

VER	DATE	REMARKS	Drawn	Checked
1	03/01/2013	Draft	FK	NC
2	08/01/2013	Final	FK	NC

DRAWING NUMBER: **9X5889/05**

SCALE		PLOT SIZE		DATUM	PROJECTION
	Not to scale		A4		

FOREWIND

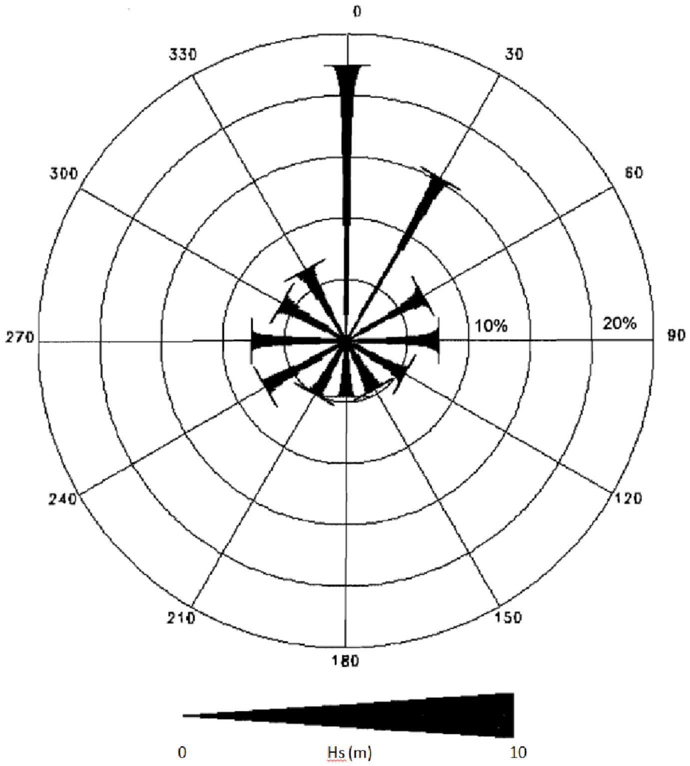

Figure 2.2a Offshore Wave Rose 1987-1995

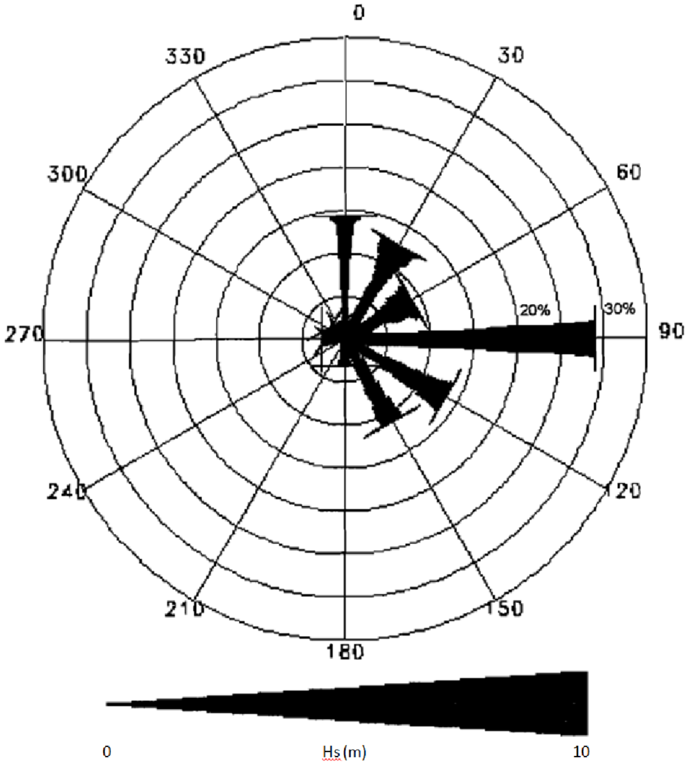

Figure 2.2b Offshore Wave Rose for Winter 1995/96

Source:
Babtie, 2000

PROJECT TITLE

DOGGER BANK TEESSIDE

DRAWING TITLE

Figure 2.2 Offshore Wave Roses

VER	DATE	REMARKS	Drawn	Checked
1	03/01/2013	Draft	FK	NC
2	08/01/2013	Final	FK	NC

DRAWING NUMBER: **9X5889/06**

SCALE	PLOT SIZE	DATUM	PROJECTION
Not to scale	A4		

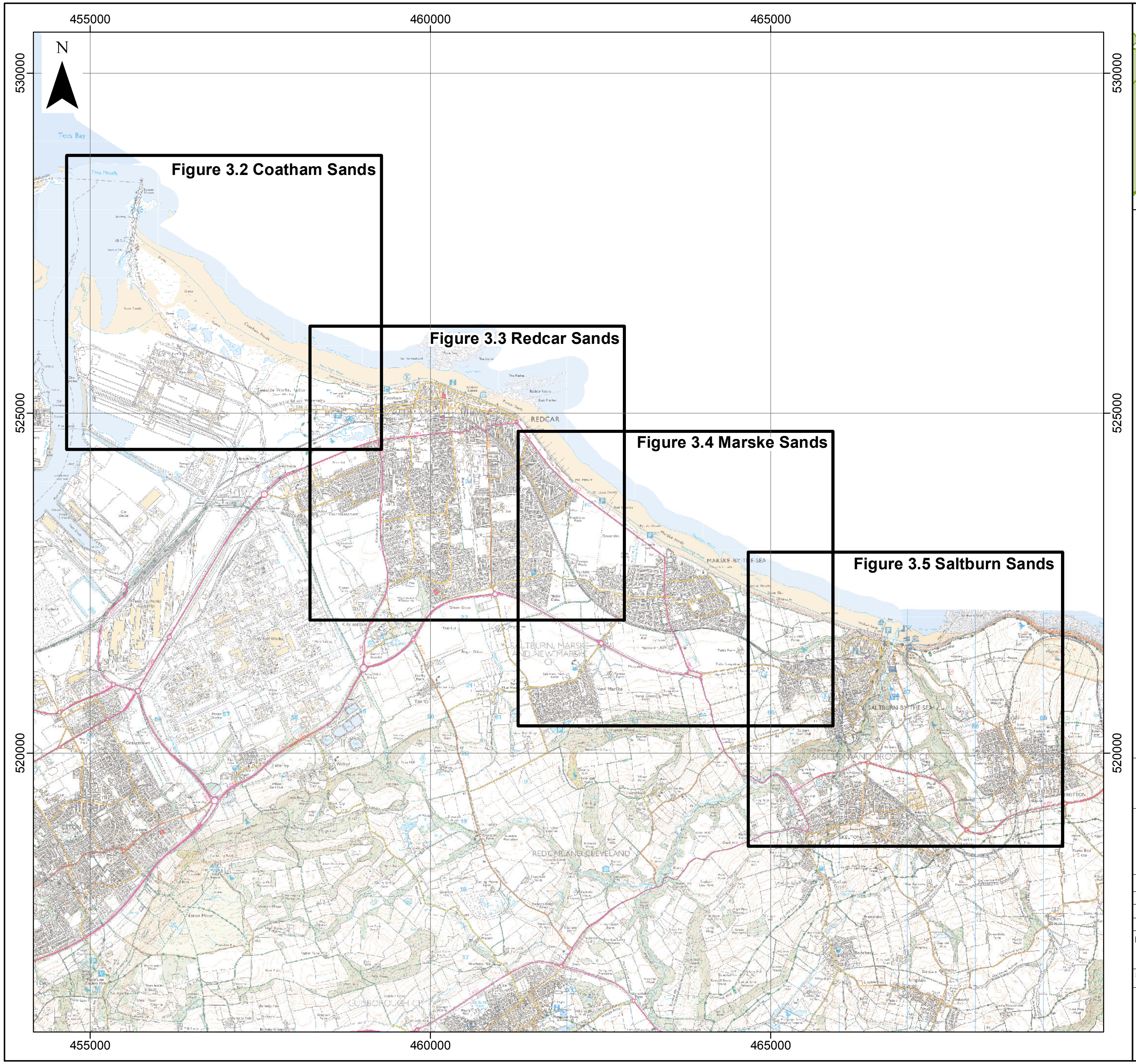

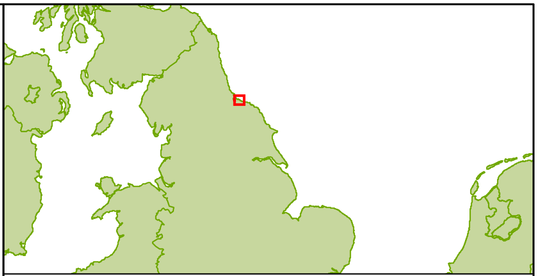

0 2
Kilometres

Source:
Ordnance Survey © Crown copyright
All rights reserved. 2012 Licence number 0100031673

PROJECT TITLE

DOGGER BANK TEESSIDE

DRAWING TITLE

Figure 3.1 Location Overview

VER	DATE	REMARKS	Drawn	Checked
1	03/01/2013	Draft	FK	NC
2	08/01/2013	Final	FK	NC

DRAWING NUMBER: 9X5889/07

SCALE	1:85,000	PLOT SIZE	A4	DATUM	OSGB36	PROJECTION	BNG

FOREWIND

Figure 4.1. The ratio of cone resistance in bars (1 bar = 0.1MPa) to the number of blows *N* in the Standard Penetration Test as a function of sediment size D_{50} (after Robertson et al., 1983)

4.3.3 The Erosion Threshold: $P_R = 0.48EI^{0.44}$ = the threshold power required to scour the material in kW/m^2

4.3.4 The seabed profile is divided into layers according to the soil characteristics obtained from the borehole logs. For each layer, an erosion threshold stream power P_R is calculated as described above. The applied stream power $P(S)$ at an elevation S below the seabed level is given by the following solution:

$$P(S) = a \cdot \exp\left(-b\frac{S}{S_{\max}}\right)P_a$$

where:

S_{max} = maximum scour depth conservatively predicted by some independent means, such as that obtained using the Khalfin (2007) solution, which is for granular sand
S = depth at the base of each layer $0 < S \leq S_{max}$
P_a = applied stream power at the seabed, in the absence of the structure (Watts/m^2)

4.3.5 The applied stream power P_a is given by:

$$P_a = \tau \cdot U$$

where:

τ = applied seabed shear stress under the action of waves and currents (N/m^2)
U = water flow velocity on the seabed (m/s)

4.3.6 For a circular structure, the coefficients a and b have the values 8.95 and 1.92 respectively, as derived experimentally and reported by Annandale and Smith (2001). It is noted that the value of a is close to the theoretical value of 8.0 for a circular cylinder.

4.3.7 A conservative approach was adopted to the assessment of the applied stream power due to the combined action of waves and currents at the seabed. For the 50-year condition, the highest applied hydraulic power across the project site was used for the value of P_a. In this context, τ_{max} was $8.3N/m^2$ and the combined wave-current maximum water particle velocity U was 3.33m/s, resulting in an applied stream power P_a of 27.5 $Watts/m^2$ at the seabed. This approach in itself is conservative, since it assumes that the stream power is constant with time, as in a stream flow, whereas in reality a large proportion of it is fluctuating, due to the contribution from the waves.

4.3.8 The results show that the predicted maximum scour depth for the 50-year storm condition using the Annandale solution for Dogger Bank Teesside A & B is approximately 4.3m (considering all of the boreholes that were located in the project) (Fugro, 2012). This revised scour depth is a factor of two less than that attributed to a pure loose granular sand model, which is 10.1m for a 50-year return period. For the one-year storm condition, the Annandale method estimated that the maximum scour depth would be approximately 2.2m, which is also around a factor of two less than that attributable to the loose granular sand model, at the same return period.

4.3.9 **Figure 4.2** shows the application of the Annandale method at the 50-year return period, to data from six example profiles reported in Fugro (2012). When the applied erosive power lies to the right of the resistance power in each plot, then the seabed will erode at that depth, due to scour. Once the applied erosive power falls to the left of the resistance data, then further scouring of the seabed is unlikely to occur beyond that depth.

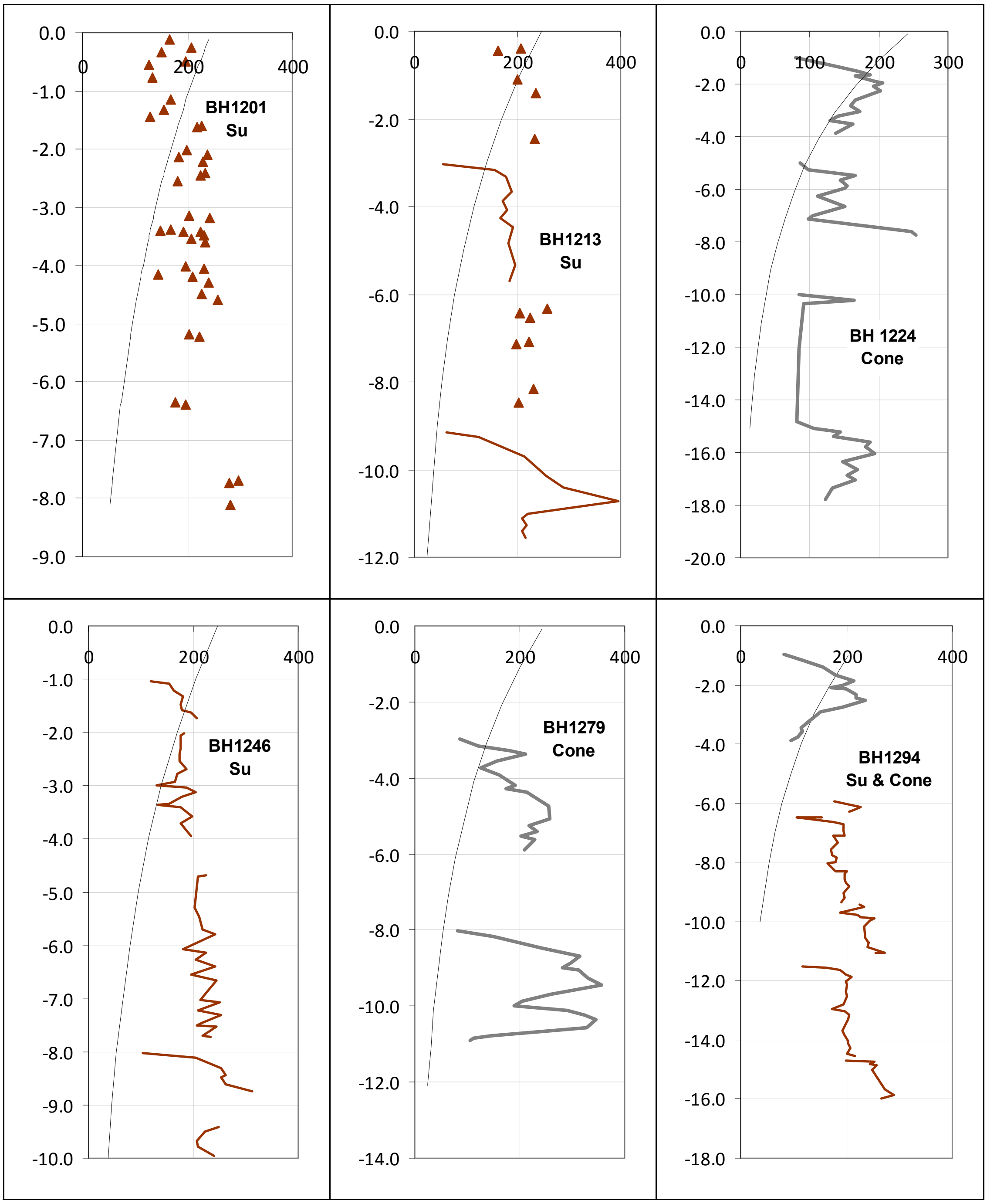

Figure 4.2. Erosion resistance power of the seabed sediment compared against the applied hydraulic scour, all in W/m^2. The irregular fine plots apply to the sand and the bold lines relate to the clay horizon. The fine regular curve represents the applied erosive power due to scouring around the structure.

4.4 Method of adjusting the scour volumes to account for the erosion-resistant clay layer

4.4.1 The Dogger Bank Formation clay horizon is beneath the sand deposits. It is characterised by Fugro (2012) as a stiff to hard clay, with typical undrained shear strength of 150kPa. It is predicted that this clay cannot be eroded by hydraulic scour and that it acts as a barrier to the progression of further erosion.

4.4.2 This section describes a model that was developed for Dogger Bank Teesside A & B, to take account of the further reductions in scour volume afforded by the existence of the clay at depth below the seabed. The model is based on field observations made at Barrow offshore wind farm (Whitehouse et al., 2011).When the clay layer was at a higher elevation than the bottom of the equilibrium scour hole obtained using the Annandale solution, then this model was applied, to derive the final equilibrium scour volume.

4.4.3 Although the clay layer (Dogger Bank Formation) will provide a defined limit to the depth of equilibrium scour around the structures, if it is sufficiently close to the surface, the exact form of the scour hole that will develop is not so clear. For Dogger Bank Teesside A & B, reference has been made to the observations reported by Whitehouse et al. (2011) at Barrow offshore wind farm, where some of the monopoles are located in sand with a scour-resistant clay subsurface, while others are in plain sand. **Figure 4.3** shows a typical comparative example from Barrow, in which the monopole on the left has no hard subsurface within easy reach of the equilibrium scour depth, whilst the structure on the right is underlain with a scour-resistant clay substratum at around 0.5m below the seabed.

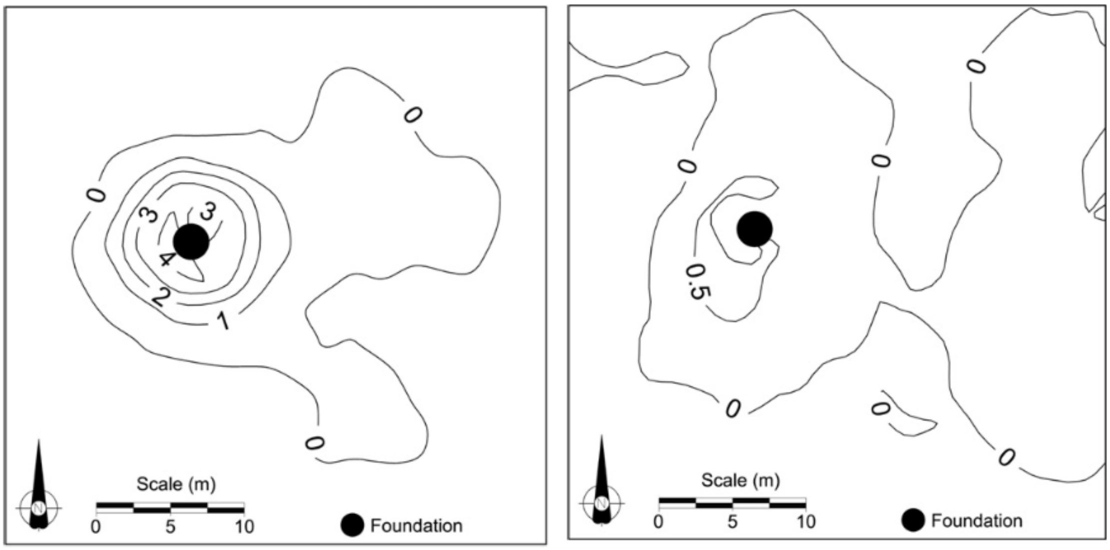

a) scour with no hard subsurface below the seabed level

b) scour with hard subsurface at~0.5m below the seabed level

Figure 4.3. Scour observations reported by Whitehouse et al. (2011) for two different monopoles at Barrow offshore wind farm

4.4.4 In the second case, the contour pattern shows that the sand has been scoured down to expose the clay subsurface at 0.5m below the seabed, and it then rises with a gentle slope, in the form of an irregular dish, back up to ambient seabed level. The general minimum distances between the zero seabed contour and the monopole are of the same order of magnitude in both cases. Using these observations as a guide, the following properties were established for the form of the scour hole that is limited by the erosion-resistant clay substratum:

- the location of the outer edge of the scour hole was taken to be the same as that which would occur in the absence of the clay substratum

- a proportion of the seabed is fully exposed down to the clay substratum, by an amount identified by the term $k \cdot S_e \cdot \mathrm{cotan}\phi$, which is the width of the full scour hole, measured radially from the face of the structure. S_e is the full equilibrium scour depth for the sand unrestrained by a clay substratum. The coefficient k is a factor less than unity; a value of 0.6 was conservatively adopted for the value of k, based upon observation of the Barrow results.

- **Figure 4.4** shows the assumptions in schematic form

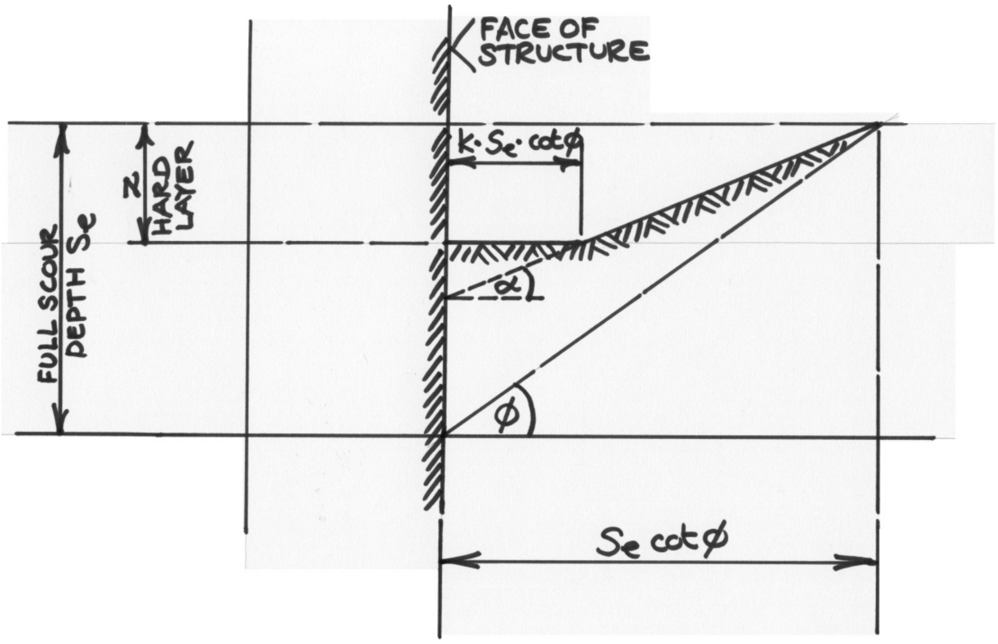

Figure 4.4. Model adopted for scour down to a resistant substratum

In **Figure 4.4**:

S_e = predicted full equilibrium scour depth in an infinite granular seabed, unrestrained by any hard substratum (m)
Z = depth of the hard substratum beneath the seabed (m)
k = coefficient less than unity, representing the proportion of the available potential seabed space (measured radially out from the face of the structure) that is scoured down to the hard substratum, leaving a horizontal platform around the structure
α = slope angle of the scoured surface beyond the horizontal platform
ϕ = angle of friction of the seabed sediment

4.5 Summary of overall method

4.5.1 Step 1: Predict the equilibrium scour depth using the granular sand assumption. This also ignores the existence of a hard clay substratum that could eventually limit the scour depth.

4.5.2 Step 2: Compare the predicted equilibrium scour depth from Step 1 against the most conservative estimate obtained by applying the Annandale solution, based on geotechnical properties in the borehole data sets. If the result from Step 1 is greater than that applying to the Annandale result, then over-write the Step 1 results with the Annandale value.

- The most conservative prediction for the 50-year scour depth for Tranche B, applying the Annandale method, is estimated to be 4.3m. This is always less than that applying to the 50-year granular assumption, and therefore the unrestrained scour depth during a 50-year event is 4.3m.

- The most conservative prediction for the one-year scour depth, applying the Annandale method, is estimated to be 2.2m. This is always less than that applying to the one-year granular assumption, and therefore the unrestrained scour depth during a one-year event is 2.2m.

4.5.3 Step 3: To execute Step 2 to a more refined level, the borehole data would be interpolated across the site and used to apply different sediment geotechnical properties to each GBS accordingly. The method used here is conservative because it takes the worst estimate of seabed shear stress due to combined waves and tides for each return period and uses that in the Annandale method, and the results from the worst case borehole data were used to estimate the equilibrium scour depth.

4.5.4 Step 4: Apply a correction to the equilibrium scour volume predicted from Steps 1 and 2, due to the existence of the scour-resistant clay layer.

Application of the Annandale solution confirms that the clay layer is scour-resistant at the one-year and 50-year return periods.

- Equilibrium scour volumes were predicted based upon an elliptical scour hole, which is truncated by the scour-resistant clay substratum, if the latter is sufficiently close to the seabed.

- It has been assumed throughout that the friction angle is 38.6° as indicated by the field data, apart from within the top 25-30cm of sediment. This friction angle value is based on geotechnical data from boreholes and is believed to be due to the existence of organic material within the sand matrix, which is acting as a binding and strengthening/densification agent.

4.5.5 **Figure 4.5** shows the cumulative distribution of predicted equilibrium scour depths across the 300 conical GBS foundations in Dogger Bank Teesside A & B, obtained using the granular sand model with no scour-resistant sub-layer, followed by the application of the Annandale method and taking account of the scour-resistant substratum; the Annandale limit is clearly shown in the left hand curve.

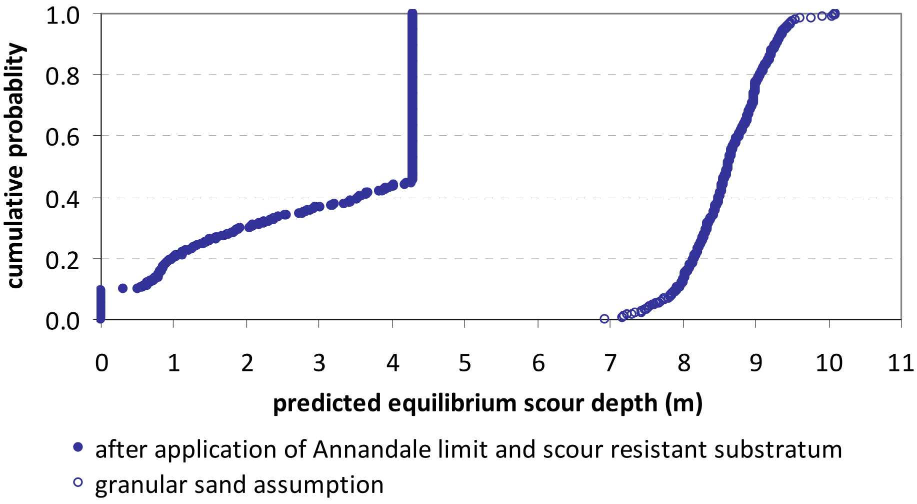

Figure 4.5. Dogger Bank Teesside A & B under 50-year storm conditions. Indicative cumulative distributions of predicted scour depths made using the granular loose sand model and after application of the Annandale limit and the use of the shear-resistant clay substratum

4.6 Comparison with scour around wrecks in Tranche A

4.6.1 Scour data at wrecks is available for five locations in Tranche A. **Table 4.1** summarises the wreck locations and their dimensions. Eight possible wrecks have been identified within Tranche B (Gardline, 2013). All identified wrecks show no real scour; however most sit within depressions of varying depths.

Table 4.1. Locations and dimensions of the five wrecks observed in Tranche A that exhibit scour (source: Wessex Archaeology)

ID	Easting (m)	Northing (m)	Length (m)	Width (m)	Height (m)
70508	441861	6078534	43.60	14.00	0.83
70505	450453	6082183	16.80	10.30	1.83
70500	416938	6099717	115.15	21.33	2.07
70501	415802	6074542	54.94	19.16	1.50
70502	445479	6072251	70.73	8.91	2.99

4.6.2 The heights of the wrecks are small compared to the mean water depths in which they are located, which range from 23m to 31m. The modest heights of the structures exert a strong influence on the maximum scour depths that can be achieved around these wrecks.

4.6.3 Predictions were made of the equilibrium scour depths that would occur under one-year conditions with currents alone and waves combined with currents to compare with the observed scour depths. The methods applied were the modified Khalfin (1983) and Bos et al. (2002b) solutions for scour around large structures by currents alone and the solution developed by Bos et al. (2002b) for scour around large submerged gravity structures in waves and currents combined. **Table 4.2** summarises the results of the equilibrium scour depth predictions compared with the observed values. In all cases, a one-year return period tidal current speed of 0.91m/s has been assumed.

Table 4.2. Observed scour depths at the wrecks and predicted values commensurate with the one-year tide and wave conditions

ID	H_s(m)	Water Depth (m)	Scour Depth (S_e)		
			Observed (m)	Predicted in currents (m)	Predicted in waves and currents combined
70508	5.78	23.1	1.2	0.56	1.64
70505	5.92	25.2	1.0	0.99	0.71
70500	6.24	31.1	1.6	1.30	1.90
70501	5.52	23.9	1.5	1.00	1.76
70502	5.84	22.6	1.4	1.99	2.60

4.6.4 The observed scour depths, with one exception (ID 70502), are either very similar to those predicted under one-year current conditions alone, or they lie between those associated with currents and those due to waves and currents combined. The observed scour depths around the wrecks have developed over a long period of time. In the scour volume predictions for the plume modelling, the prediction of released volume is based upon the assumption of a one-off storm event of sufficient magnitude to mobilise the full scour depth, taking account of the strength of the seabed sediment. Over a very long period of time around wrecks, the scour hole can be enhanced and deepened by the repeated re-working and softening of the seabed sediment caused by intermittent hydraulic action. For that reason, the granular assumption might be closer to reality for very long-term scour effects. The object of the present study was to predict the effects of plume dispersion from scour caused by a single extreme storm.

4.6.5 A larger sample of wreck scour data is required in order to make more definitive judgements. However, it appears that the use of one-year return period conditions in conjunction with the wreck dimensions and scour theory results in reasonable agreement between observations and predictions of scour.

4.6.6 The observed scour depths are typical of what could be expected of structures with these dimensions. However, the predictions apply to submerged structures of low height relative to the depth of the water column. Surface-piercing gravity base structures can be expected to generate significantly deeper scour.

4.7 Empirical methods used to predicted natural background suspended sediment concentration for one-year and 50-year storms

4.7.1 The natural background suspended sediment concentration that could be expected to arise during an extreme condition of waves and currents was estimated using the methods recommended by Soulsby (1997) and augmented for wave-current interaction using the solution developed by Soulsby and Clarke (2005). The objective of this exercise was to place the predicted volumes released by the scour process into the context of the scale of natural processes. It was also necessary to address whether there is sufficient mobile sediment available on the seabed in order to sustain the predicted natural suspended volumes.

4.7.2 Using the approach adopted by Soulsby (1997), the form of concentration profile under the joint action of waves and currents may be typified by expressions such as:

$C(z)=C_a\left(\frac{z}{z_a}\right)^{-b_{\max}};z_a \le z \le z_w$ $C(z)=C(z_w)\left(\frac{z}{z_a}\right)^{-b_m};z_w < z \le h$	$b_{\max}=\frac{w_s}{\kappa \cdot u_{*,\max}}$ $b_m=\frac{w_s}{\kappa \cdot u_{*,m}}$
$z_w=\frac{u_{*,\max}T}{2\pi}$ wave boundary layer thickness	

where:

z = height above the seabed (m)
$C(z)$ = sediment concentration at height z
C_a = reference concentration at height z_a
z_a = reference height near seabed (m)
$C(z_w)$ = concentration at $z = z_w$
w_s = settling velocity (m/s)
κ = von Karman constant (0.4 in value)
$u_{*,max} = (\tau_{max}/\rho)^{1/2}$ maximum shear velocity (m/s)
$u_{*,m} = (\tau_m/\rho)^{1/2}$ mean shear velocity (m/s)
τ_{max} = maximum bed shear stress during the wave cycle (N/m^2)
τ_m = mean bed shear stress during the wave cycle (N/m^2)
T = wave period (s)

4.7.3 Soulsby (1997) recommended that the formula developed by Zyserman and Fredsøe may be applied to obtain the reference concentration:

$$C_a=\frac{0.331(\theta_{\max}-0.045)^{1.75}}{1+0.72(\theta_{\max}-0.045)^{1.75}} \text{ at height } z_a = 2D_{50}$$

4.7.4 In the above expression, θ_{max} is the Shields parameter applying to the maximum shear velocity. This is an adaptation of the Zyserman and Fredsøe solution, recommended by Soulsby (1997); if sediment concentration in currents alone were being considered, θ_{max} would be replaced by the critical Shields parameter θ_S.

4.7.5 For both the one- and 50-year return period wave parameters, it is predicted that wash-out conditions on the seabed will prevail; the bed will be scoured flat and no sand waves will be formed at the peak of the storm. This is primarily due to the combination of long wave periods and also wave heights that are large in relation to the average water depths.

4.7.6 The maximum and mean shear velocities have to be predicted in order to implement this solution. Soulsby (1997) used what he referred to as the *Data13* solution, which has tabulated coefficients. For the purpose of this analysis, the maximum and mean shear velocities were predicted using the more recent method developed by Soulsby and Clarke (2005).

5 REFERENCES

Annandale, G. and Smith, S. 2001. Calculation of bridge pier scour using the Erodibility Index Method. Report No. CDOT-DTD-R-2000-9, U.S. Department of Transportation.

Annandale, G. 1995. Erodibility. Journal of Hydraulic Research, 33,471-494.

Annandale, G. 2006. Scour Technology: Mechanics and Engineering Practice. Mc Graw-Hill Civil Engineering.

Bolle, A., Haerens, P., Trouw, K., Smits, J. and Dewaele, G. 2009. Scour around gravity-based wind turbine foundations – prototype measurements. In: Coasts, Marine Structures and Breakwaters. Adapting to Change (Ed.Allsop, W.), 103-118, Thomas Telford Books, London.

Bolle, A., Mercelis, P., Goossens, W. and Haerens, P. 2010. Scour monitoring and scour protection solution for offshore gravity based foundations. Proceedings of the Fifth International Conference on Scour and Erosion, San Francisco, 7-10thNovember 2010. Geotechnical Special Publication 120, ASCE.

Bos, K.J., Veheij, H.J., Kant, G. and Kruisbrink, A.C.H. 2002a. Scour Protection around Gravity Based Structures Using Small Size Rock. Proceedings of First International Conference on Scour of Foundations, Texas, 17-20th November, 2002.

Bos, K.J., Chen, A., Verheij, H.J., Onderwater, M. and Visser, M. 2002b. Local Scour and Protection of F3 Offshore GBS Platform. Proceedings of the 21st International Conference of Offshore Mechanics and Arctic Engineering, Oslo, June 23-28th.

Eadie, R.W. and Herbich, J.B. 1986. Scour about a single, cylindrical pile due to combined random waves and a current. Proceedings of the Coastal Engineering Conference, 1858–1870.

Fugro.2012. Technical Note – parameter plates for Design Basis (Borehole data) – Dogger Bank Tranche B. September, 2012.

Harris, J.M., Whitehouse, R.J.S. and Benson, T. 2010a. The time evolution of scour around offshore structures. Proceedings of the Institute of Civil Engineers, Maritime Engineering, 163,3-17.

Hoffmans, G.J.C.M. and Verheij, H.J. 1997. Scour Manual. A.A. Balkema, Rotterdam.

Khalfin, I.S.H. 1983Local scour around ice-resistant structures caused by waves and current effect. P.O.A.C. Symposium 28, Helsinki, Volume 2,992-1002.

Khalfin, I.S.H. 2007. Modelling and calculation of bed score around large-diameter vertical cylinder under wave action. Water Resources, 34, 49-59.

Khalfin, I.S.H., Avdeewa, V.I. and Longiniv, V.V. 1988. Local scour of riprap around ice-resistant cylindrical and conical gravity structures caused by waves. Proceedings of the International Conference on Technology for Polar Areas (POLAR-TECH-88), Trondheim, Volume I,275-285.

Larsen, B.J. and Frigaard, P. 2005. Scour and scour protection for wind turbine foundations for the London Array. University of Aalborg Coastal Engineering Report, 17.

Robertson, P.K., Campanella, R.G. and Wightman A. 1983. SPT-CPT correlations. ASCE Journal of Geotechnical Engineering, 109, 1449-1459.

Soulsby, R. L. 1997. Dynamics of Marine Sands. Thomas Telford Publications.

Soulsby, R.L. and Clarke, S. 2005. Bed shear stresses under combined waves and currents on smooth and rough beds. HR Wallingford Report TR137.

Sumer, M. B. and Fredsϕe, J. 2002. The Mechanics of Scour in the Marine Environment. World Scientific.

Whitehouse, R.J.S. 2004. Marine scour at large foundations. In. Proceedings of the Second International Conference on Scour and Erosion, Singapore, November 2004 (Eds. Chiew, Y-M., Lim, S-Y. and Cheng, N-S), 455-463.

Whitehouse, R.J.S., Harris, J. and Sutherland, J. 2010. Evaluating scour at marine gravity structures. First European IAHR Congress, Edinburgh, 4–6th May, 2010.

Whitehouse, R.J.S., Harris, J.M., Sutherland, J. and Rees, J. 2011. The nature of scour development and scour protection at offshore windfarm foundations. Marine Pollution Bulletin, 62, 73-78.